Inês Mendes de Andrade Araújo de Sousa

Life history parameters and valorisation of a low commercial value fish species: the case study of piper gurnard, *Trigla lyra* Linnaeus 1758

UNIVERSIDADE DO ALGARVE

Faculdade de Ciências e Tecnologia

2019

Inês Mendes de Andrade Araújo de Sousa

Life history parameters and valorisation of a low commercial value fish species: the case study of piper gurnard, *Trigla lyra* Linnaeus 1758

Mestrado em Biologia Marinha

Supervisor:

Vera Sequeira

Co-supervisor

José Pedro Andrade

UNIVERSIDADE DO ALGARVE

Faculdade de Ciências e Tecnologia

2019

Título: Life history parameters and valorisation of a low commercial value fish species: the case study of piper gurnard, *Trigla lyra* Linnaeus 1758

Declaração de autoria de trabalho

Declaro ser a autora deste trabalho, que é original e inédito. Autores e trabalhos consultados estão devidamente citados no texto e constam da listagem de referências incluída.

_____

Direitos de cópia ou Copyright

© Copyright: Inês Mendes de Andrade Araújo de Sousa

A Universidade do Algarve reserva para si o direito, em conformidade com o disposto no Código do Direito de Autor e dos Direitos Conexos, de arquivar, reproduzir e publicar a obra, independentemente do meio utilizado, bem como de a divulgar através de repositórios científicos e de admitir a sua cópia e distribuição para fins meramente educacionais ou de investigação e não comerciais, conquanto seja dado o devido crédito ao autor e editor respetivos.

Agradecimentos

Em primeiro lugar, quero agradecer a toda a equipa que me acompanhou durante o meu trabalho no laboratório. Obrigada à Ana, à Ana Rita, ao Prof. Leonel e à Vera, pela sua ajuda, apoio e amizade, por responderem sempre às minhas dúvidas e por acreditarem no meu trabalho. Foram fundamentais para que tudo corresse bem e fizeram com que este ano que passou valesse a pena. Em particular:

- Ao Prof. Leonel, por toda a experiência e conhecimento que partilhou comigo.

- À Ana Rita, por toda a ajuda com os otólitos.

- À Ana, por toda a ajuda com a estatística.

- À Vera, que é a minha orientadora, pela oportunidade que me deu em fazer a minha tese no laboratório e em fazer parte da equipa, pela sua amizade, disponibilidade, ensinamentos, colaboração e ajuda na elaboração da tese.

Também gostaria de agradecer ao meu coorientador, José Pedro Andrade, pela sua disponibilidade mesmo estando longe, pela experiência que me passou e pela sua contribuição na revisão da tese.

Um grande agradecimento aos meus amigos e colegas do mestrado, que foram o meu porto de abrigo durante o primeiro ano, em que estive longe de casa. Obrigada à Kris, ao Antonio, à Raquel, à Catarina, à Mariana, à Marta e à Taina, pelos grandes momentos, risos, almoços na cantina e horas de estudo na biblioteca. Também agradeço aos meus amigos em Lisboa, que me encorajaram na minha escolha em estudar Biologia Marinha e cuja amizade está sempre presente.

Por último, quero agradecer à minha família, que são o meu apoio e o meu refúgio, sempre. Um especial agradecimento:

- À Flávia, ao Leonel, à Cristina e ao Sr. Zé, por quererem sempre o melhor para mim e pelo seu afecto e amizade.

- Aos meus avós e tios, por todos os momentos que partilhamos desde sempre e por estarem ao meu lado. Mesmo longe, estão sempre no meu pensamento.

- Aos meus irmãos, Ana Luísa e Miguel, por serem os melhores irmãos do mundo e aqueles com quem eu sei que posso contar.

- À minha mãe e ao meu pai, pelo seu amor, pelo seu sacrifício em me proporcionarem tudo o que tenho e fazerem de mim o que sou hoje. Por me darem a possibilidade de estudar aquilo que gosto e mais ainda de estudar longe de casa. Esta tese é dedicada a eles.

- Ao meu namorado, Zé Miguel, o meu melhor amigo, parceiro de todos os dias e refúgio, a quem nunca conseguirei agradecer tudo o que faz por mim. Por ser o primeiro a encorajar-me, por nunca me deixar desistir e por nunca me desiludir. Juntos somos mais fortes.

Abstract

Many fishing activities involve high discarding rates constituting, a major problem for the marine ecosystem. *Trigla lyra* presents low commercial value in Portuguese landings and is mainly caught as accessory species in trawls, trammel nets, traps and pots. Published information on this species in Portuguese waters is scarce. So, the main objectives of the present study are to contribute to the knowledge of biological, namely age and growth and reproduction, and chemical parameters of *T. lyra*. Approximately 30 specimens were collected monthly from fishing vessels operating off Peniche (West coast of Portugal). The study of age and growth involved age estimation using whole *sagitta* otoliths, marginal increment ratio (MIR) and otolith edge type analysis, determination of length-weight relationship and estimation of parameters of the von Bertalanffy growth model. Regarding reproduction, the structure of the gonads was studied, and reproductive strategy was characterized, including the definition and duration of spawning season and determination of fecundity type. Chemical composition of the muscle was determined in terms of moisture, ash content, protein content, total fat and profile of fatty acids. MIR and otolith edge type analysis suggest that a single set of translucent and opaque increments is formed every year in *T. lyra* otoliths. There was a lack of small individuals in the sample, leading to the application of three adjustment methods for estimating growth parameters, with back-calculation being the best method. Sex ratio analysis indicated higher abundance of females in relation to males. Spawning season occurred between November and February and fecundity type was found to be determinate. The species proved to be beneficial regarding protein content but especially regarding fatty acid content, with the results indicating high EPA and DHA concentrations. The present study contributed to improve the knowledge on biological and chemical parameters of *T. lyra* in Portuguese waters, essential for its exploration and future valorisation.

Keywords: Portuguese coast, *Trigla lyra*, age and growth, reproduction, chemical composition.

Resumo

Em geral, a pesca está associada a taxas de rejeições mais ou menos elevadas. A rejeição corresponde à parte da captura que é trazida para bordo da embarcação de pesca, mas que é posteriormente devolvida ao mar morta ou viva. As razões associadas a rejeição prendem-se com motivos pessoais, económicos ou legais, sendo as causas mais comuns o baixo ou nenhum valor comercial da espécie capturada, a má condição do pescado (rápida deterioração ou corpo danificado), restrições em termos de tamanho mínimo, existência de quotas, TACs ou proibições de capturas acessórias, ou ainda a falta de espaço de armazenamento a bordo da embarcação de pesca.

Os ruivos são espécies que ocorrem ao longo da costa Portuguesa e que são capturadas como espécies acessórias em redes de arrasto, redes de emalhar e de tresmalho e armadilhas. Podem ser rejeitadas no mar ou desembarcadas em lota, apresentando um baixo valor comercial. Entre elas, *Trigla lyra*, conhecida como cabra-lira, é uma das espécies de ruivos mais desembarcada. É uma espécie bentónica, pouco estudada em termos biológicos em Portugal, sendo que a maior parte da informação existente se refere ao Mar Mediterrâneo.

O presente estudo pretende contribuir para um maior conhecimento de alguns parâmetros biológicos e químicos de *T. lyra*, nomeadamente a idade e crescimento, a reprodução e a composição química.

Aproximadamente 30 indivíduos foram recolhidos mensalmente entre Maio de 2018 e Maio de 2019, por embarcações de pesca de arrasto, de redes de emalhar e tresmalho e de armadilhas, a operar ao largo de Peniche (costa Oeste de Portugal). No laboratório, foram recolhidos dados individuais relativos ao comprimento e peso total, removidas as gónadas e restantes órgãos da cavidade abdominal, registado o peso eviscerado, o peso da gónada e o peso do fígado. O estudo da idade e crescimento envolveu a estimativa de idades através da análise de otólitos *sagitta* inteiros e a sua validação recorrendo à análise da evolução do bordo do otólito e do incremento marginal ao longo dos meses de amostragem. Foi determinada a relação comprimento-peso e os parâmetros de crescimento da espécie foram estimados utilizando o modelo de crescimento de von Bertallanffy. Devido à sub-representação na amostra de indivíduos com comprimento total inferior a 23 cm, foram utilizados três métodos de ajuste ao modelo de crescimento: otólito inteiro, retro cálculo e método combinado. O estudo da estratégia reprodutiva

envolveu a determinação da proporção dos sexos, a caracterização do aspecto macroscópico e histológico das gónadas incluindo a identificação dos tipos celulares sexuais e medição do seu diâmetro, a definição da época de reprodução e sua duração tendo por base a evolução mensal da frequência das fases de maturação do ciclo sexual bem como dos índices gonadossomático, hepatossomático e factor de condição. O tipo de fecundidade da espécie foi avaliado tendo em conta os quatro critérios estabelecidos em literatura relativamente à distribuição ao longo dos meses dos ovócitos em vitelogénese avançada no ovário, variação do seu número e diâmetro e percentagem de atrésia ao longo dos meses. A composição química no músculo foi determinada em termos de humidade e teor de cinza, com base nas normas portuguesas, de teor proteico através do método de Kjeldahl, de teor de gordura através do método de Folch e de perfil de ácidos gordos através de cromatografia em fase gasosa.

Os resultados demonstraram diferenças nas distribuições frequência-comprimento entre machos e fêmeas, alcançando as fêmeas maiores comprimentos que os machos. O comprimento e idade máximos das fêmeas foram de 45.1 cm e 12 anos, respectivamente, enquanto que o comprimento e idade máximos dos machos foram de 41.0 cm e 10 anos, respectivamente. No estudo da idade e crescimento, a análise da evolução mensal do incremento marginal bem como do bordo do otólito indicaram que os incrementos são depositados anualmente. A relação comprimento-peso revelou a inexistência de diferenças significativas no crescimento entre os dois sexos e que a espécie possui um crescimento isométrico. Quanto aos parâmetros de crescimento, o retro cálculo revelou melhor ajuste ao conjunto dos dados, tendo-se obtido valores de $L\infty$ de 42.579 cm, de k de 0.204 e de t_0 de -1.455. Relativamente à reprodução da cabra-lira, a estrutura das gónadas revelou a presença de todos os estados de desenvolvimento de ovócitos e de células sexuais masculinas. A proporção dos sexos indicou que as fêmeas foram mais abundantes do que os machos em quase todos os meses de amostragem, incluindo os meses da época de reprodução, que foi definida como o período entre Novembro e Fevereiro. A evolução do índice gonadossomático ao longo dos meses corroborou a definição da época de postura, uma vez que os valores mais altos se verificaram no período acima indicado. O tipo de fecundidade de *T. lyra* foi classificado como determinado, uma vez que se verificou a presença de hiato entre a população de ovócitos não vitelados e vitelados, a diminuição do número de ovócitos em vitelogénese avançada e um aumento do seu diâmetro ao longo dos meses, assim como a inexistência de atrésia

massiva no final da época de postura. Em termos de estratégia reprodutiva, os resultados sugerem que a espécie apresenta fertilização externa, é gonocorística, apresenta um desenvolvimento dos ovócitos do tipo grupo-síncrono e a desova é seriada ao longo da época de postura. No que diz respeito à composição química, o componente principal do músculo de *T. lyra* foi a água, seguido pelas proteínas, cinzas e lípidos. A composição em lípidos sugere que a espécie é magra. A análise do perfil de ácidos gordos permitiu identificar 21 tipos, com uma maior concentração de ácidos gordos polinsaturados. Entre os ácidos gordos saturados, o mais abundante foi o ácido palmítico, e entre os ácidos monoinsaturados o mais comum foi o ácido oleico. Os ácidos DHA e EPA destacaram-se entre os ácidos polinsaturados. Os resultados permitiram concluir que a cabra-lira constitui uma boa fonte de proteínas e ácidos gordos sendo benéfica para consumo humano.

Em resumo, o presente estudo contribuiu para um melhor conhecimento dos parâmetros de história de vida de *T. lyra*, nomeadamente da idade, do crescimento e da reprodução, informação fundamental para uma correta gestão da exploração da espécie em Portugal. A análise da composição química permitiu conhecer as suas características nutricionais e, assim, avançar na valorização futura da espécie enquanto recurso pesqueiro, passando por exemplo por um melhor aproveitamento do recurso e criação de novos produtos ao consumo, o que pode ser importante, já que *T. lyra* é uma espécie, presentemente, com baixo valor comercial em Portugal.

Palavras-chave: Costa Portuguesa, *Trigla lyra*, idade e crescimento, reprodução, composição química.

Index

Figures Index

Tables Index

Abbreviations

A - Atresia

AA - Arachidonic acid.

ALA - α-linoleic acid

An - Anterior region

APE - Average percent error

AS - Actively spawning

AR - *Antirostrum*

CA - Cortical alveolar oocyte

c-AIC - Akaike's information criterion corrected for small samples

CFP - Common Fisheries Policy

CV - Coefficient of variation

D - Index of precision

De - Developing

Df - Degrees of freedom

DHA - Docosahexaenoic acid

Do - Dorsal edge

DPA - Docosapentaenoic acid

EPA - Eicosapentaenoic acid

EW - Eviscerated weight

FAME - fatty acid methyl ester

GC-FID - Gas Chromatography – Flame Ionization Detector

GSI - Gonadosomatic index

GW - Gonad weight

GVM - Germinal vesicle migration

H - Hydrated oocyte

HPLC - High performance liquid chromatography

HSI - Hepatosomatic index

I - Immature

K - Fulton's condition factor

k - growth parameter

L - Lobule

Li - Liver

LA - Linoleic acid

LW - Liver weight

L_{∞} - Mean asymptotic length

MIR - Marginal increment ratio

MUFAs - Monounsaturated fatty acids

NP - "Norma Portuguesa"

OM - Oocyte maturation

P - Posterior region

PG - Primary growth oocyte

POFs - Post-ovulatory follicles

PUFAs - Polyunsaturated fatty acids

R - *Rostrum*

RG - Regressing

RN - Regenerating

S - *Sulcus acusticus*

Sc - Spermatocytes

SC - Spawning capable

SD - Standard deviation

SFAs - Saturated fatty acids

Sg - Spermatogonia

St - Spermatids

Sp - Spermatocyst

Sz - Spermatozoids

t - tons

t_0 - Theoretical age at which the length of the fish is zero

TAC - Total allowable catches

T - Testes

TL - Total length

TW - Total weight

V - Ventral edge

<Vtg3 - Primary and secondary vitellogenic oocyte

Vtg3 - Tertiary vitellogenic oocyte

YC - Yolk coalescent

χ^2 - Chi-square test statistic

1. Introduction

1.1. Discards in fisheries

Discards associated with fisheries are a reason of great concern among scientists and other stakeholders around the world. Most fishing activities involve high discarding rates of about 30 million tons of the total marine fish caught by world fisheries, in a year (corresponding to 110-130 million tons) (Nellemann et al., 2009). Discards correspond to the part of the catch brought aboard the fishing vessel but subsequently thrown back into the sea dead or alive due to personal, economic or legal reasons (Hill and Wassenberg, 1990; Alverson et al., 1994; Hall, 1996). The most common causes are associated with low or lack of commercial value of the species caught, fish in bad conditions (deteriorates rapidly, poisonous, or damaged in some part of the body), species with some legal catch restrictions [minimum legal landing sizes, quotas or total allowable catches (TAC), or bycatch prohibitions] (Borges, 2015), or insufficient storing space aboard the fishing vessel (Hall et al., 2000). The characteristics of fishing gears also influence the discarding rates, namely their selectivity that is determined by the mesh size and type of mesh (square, hexagonal, diamond-shaped) (Hall, 1996). For example, demersal trawling has much lower selectivity than handlining, catching a great number of species that are not of interest for the fishermen and leading to a high rate of discarding (Hall et al., 2000; Kelleher, 2005).

Discarding and bycatch have numerous, mostly undesirable consequences (Bellido et al., 2011). In terms of ecological impacts, discarding affects negatively marine biodiversity and community structure, has detrimental effects on the stocks of commercially important species and leads to the decline of species taken up as bycatch (fish, cetaceans, sea turtles, seabirds, sharks) (Hall and Mainprize, 2005). Furthermore, the rejection at the surface of the sea of demersal fish caught in demersal fisheries may cause oxygen depletion due to the decomposition of discards, affecting community structure (Clucas, 1997; Hall et al., 2000). Economically, discarding offers no benefit to fishers, representing additional mortality that could be avoid (Bellido et al., 2011).

In the European Union (EU), fisheries management is controlled by the European Commission, which establishes limits and regulations, including the discarding policy. Nowadays, discarding a part of the catch is allowed and sometimes mandatory, for species with a conservation value that cannot be caught. However, in 2015, the obligation of landing (discard ban) all the catches subject to legal catch limits (minimum landing sizes,

quotas and total allowable catches) was introduced by the latest reform of the EU's Common Fisheries Policy (CFP) (EU, 2013). This policy is being progressively implemented in the European Union, including Portugal, and has the objective of improving the sustainability of fishing and the end of discards of commercially exploited species (Borges, 2015; Guillen et al., 2018). Besides this obligation, some species with no or reduced commercial value are still thrown back to the sea. The last ones may be rejected if they are occupying space aboard the fishing vessel that could be necessary to store other species with higher commercial value (Clucas, 1997), constituting a waste of resources that could be consumed or used in other applications. On the other hand, species with low commercial value, when are landed in the auctions, have low valorisation and low demand. Therefore, there is an increasing demand for studying the potential of valorisation and exploration of these species.

1.2. Gurnards

The gurnards, also known as sea robins ("ruivos", in Portuguese), are medium-sized demersal fishes that are found in all oceans, both in tropical and temperate regions. There are nine species occurring along the Portuguese coast (scientific name, common name in English, common name in Portuguese): *Peristedion cataphractum* (armed gurnard, "cabra-de-casca"), which belong to Peristediidae family; *Chelidonichthys cuculus* (red gurnard, "cabra-vermelha"), *Chelidonichthys lucerna* (tub gurnard, "cabra-cabaço"), *Chelidonichthys obscurus* (longfin gurnard, "cabra-de-bandeira"), *Chelidonichthys lastoviza* (streaked gurnard, "cabra-riscada"), *Eutrigla gurnardus* (grey gurnard, "cabra-morena"), *Trigla lyra* (piper gurnard, "cabra-lira"), *Lepitotrigla dieuzeidei* (spiny gurnard, "ruivo-espinhoso"), *Lepidotrigla cavillone* (large-scaled gurnard) which belong to the Triglidae family (Whitehead et al., 1986).

Many of these species are discarded by Portuguese fisheries (Borges et al., 2001; Olim and Borges, 2006). However, if they are not discarded, gurnards have a low commercial value given the commercial price registered in Peniche that varies between 0.45 €/Kg and 3.10 €/Kg (I. Sousa, personal observation). According to Statistics Portugal (2018), from 2007 to 2017, an annual average of 385 tons of gurnards was landed in Portugal with almost all landings (384 tons) occurring in mainland; landings have remained stable during this period (Fig.1.1). Gurnards are mostly caught as accessory species in trawls, trammel nets, traps and pots. In Portuguese fishing auctions, there is no distinction

between the species of gurnards. When landed, they have two possible designations: "ruivo" or "cabra-vermelha". The first designation is applied to bigger individuals of *C. lucerna,* whereas the second designation is applied to individuals of *T. lyra.* The remaining species may be designated as "ruivo" or "cabra-vermelha" depending on the person that is weighting the fish in the auction (I. Sousa, personal observation).

In North-East Atlantic fishing auctions, the gurnards were classified in a single category of "gurnards" until 2010. In this geographical area, gurnards are mostly caught as accessory species in multispecies trawl nets including demersal nets, and a large part of the catches is discarded aboard the fishing vessels (ICES, 2012).

Despite the low value attained in Portugal, species from Triglidae family have more commercial interest in the Mediterranean Sea, where they occur in the upper zones of the continental shelf (Papaconstantinou and Farrugio, 2000). In Greece, for example, *T. lyra* along with *C. lucerna*, are the most important Triglidae species in the fish markets (Papaconstantinou et al., 1992).

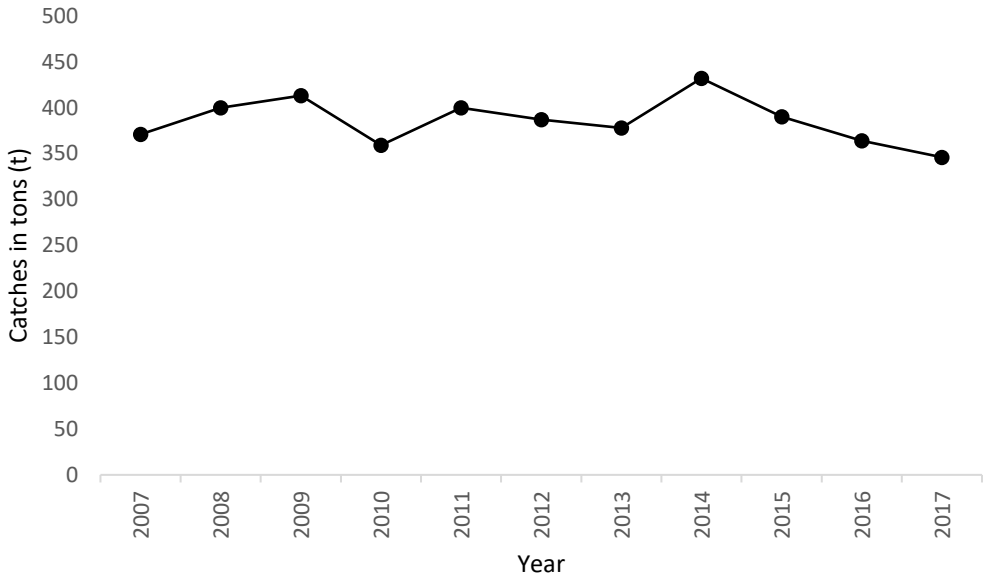

Fig.1.1. Catches of gurnards in national ports, expressed in tons (t), from 2007 to 2017 [adapted from Statistics Portugal (INE, 2018)].

1.3. Case-study species

Trigla lyra (piper gurnard, cabra-lira) is a benthonic fish that occurs in muddy, gravel and rocky bottoms at a depth of 10 to 700 m, but is usually found above 400 m. This species is distributed in Eastern Atlantic from North Sea and North of British Isles to Walvis Bay, Namibia, including Madeira and Cape Verde archipelagos, and in the Mediterranean Sea except Black Sea (Whitehead et al., 1986) (Fig.1.2). It presents elongated body, a large armored head with ridges and spines, and a cleithral spine very long and strong above the pectoral fin (Fig. 1.3). *T. lyra* feeds on crustaceans, echinoderms, molluscs, and other fish (Fischer et al., 1987).

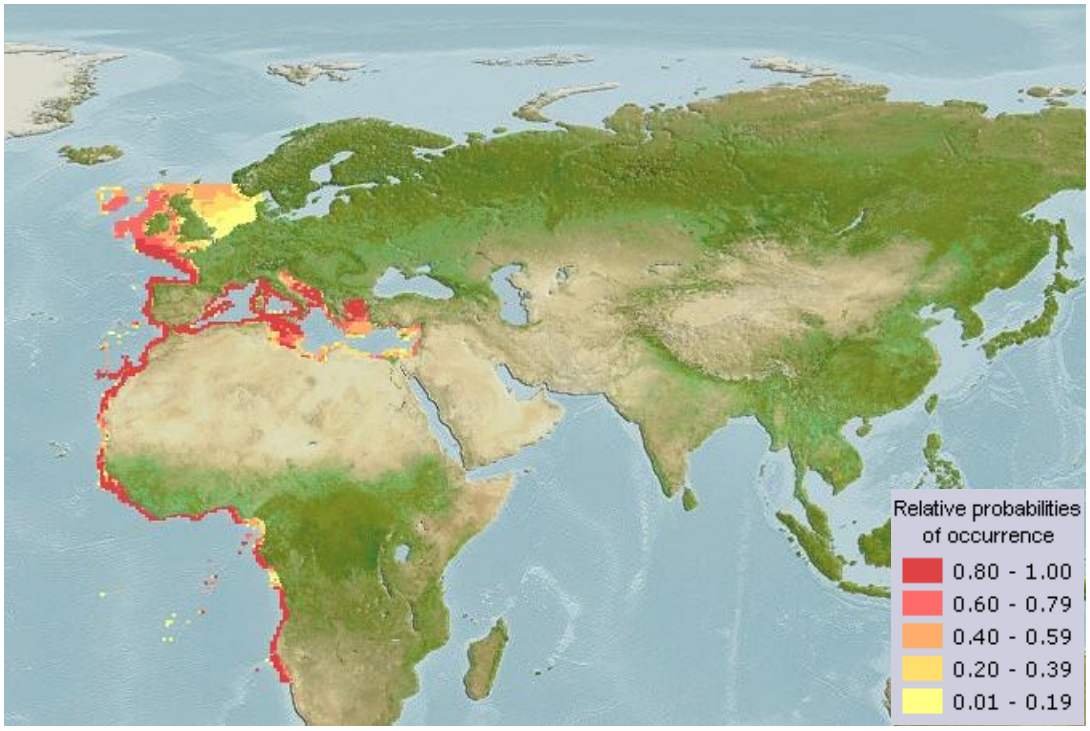

Fig. 1.2. Distribution of the piper gurnard (*Trigla lyra* Linnaeus 1758) (from AquaMaps website. Url: https://www.aquamaps.org/receive.php?type_of_map=regular).

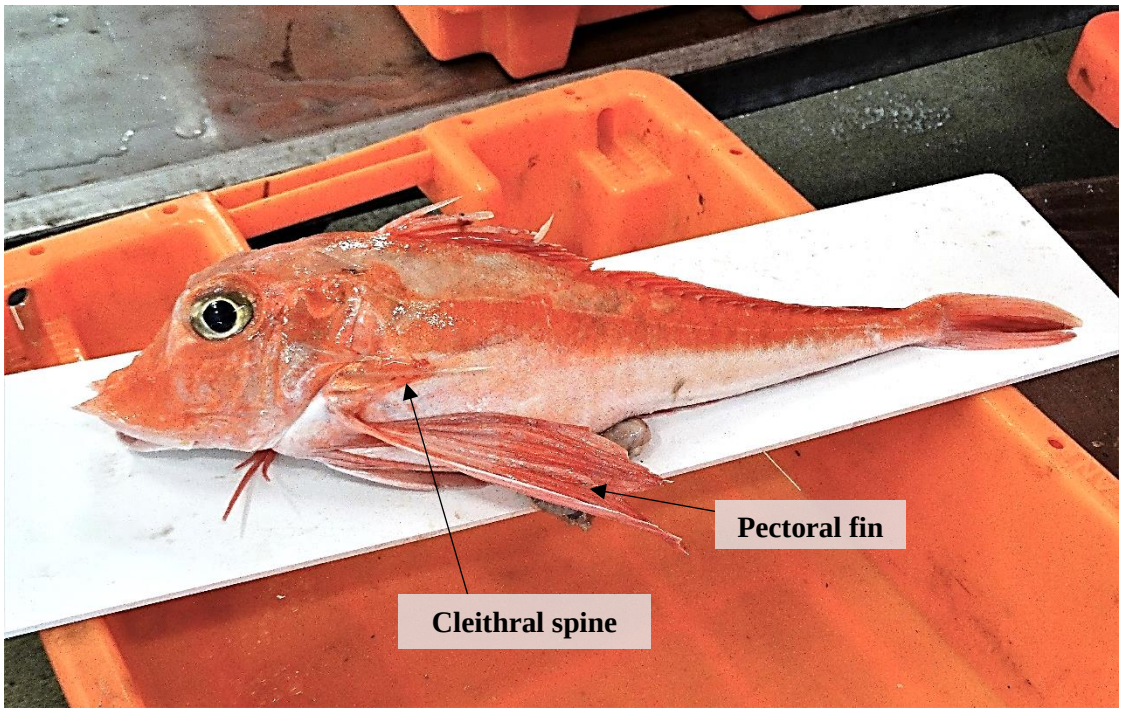

Fig. 1.3. Specimen of *Trigla lyra*, presenting a very long and strong cleithral spine above the pectoral fin.

Published information on *T. lyra* is scarce and refers mainly to the Mediterranean Sea, although there are some studies for Portugal. Previous investigations on the age and growth addressed length-frequency distribution, age estimation and age-length keys, estimated the growth parameters of the von Bertalanffy growth model and determined length-weight relationship for the Saronikos Gulf (Greece) (Papaconstantinou, 1981) and Aegean Sea (Papaconstantinou et al., 1992). Papaconstantinou et al. (1992) also estimated mortality and yield per recruit for *T. lyra*. Length-weight relationship of *T. lyra* was determined for the south coast of Portugal (Olim and Borges, 2006). Assis (2000) assessed the morphology of *sagitta*, *asteriscus* and *lapillus* otoliths of *T. lyra* for the Portuguese coast. In terms of reproduction, determination of the sex ratio and spawning season was also carried out for the Aegean Sea (Papaconstantinou et al., 1992). Muñoz et al. (2002) described the morphology of the gonads and gametogenesis of *T. lyra* and defined the spawning season of the species in the Costa Brava (North-Western Mediterranean). Papaconstantinou (1983) also studied sex ratio and reproduction period of *T. lyra* in Greek Seas. Feeding habits of the species were studied in the Saronikos Gulf (Greece) (Caragitsou and Papaconstantinou, 1994) and in the Aegean Sea (Içemer et al., 2002). The chemical composition of *T. lyra* regarding DHA, EPA, phospholipid and

cholesterol contents was analyzed by Loukas et al. (2010) in individuals from the Mediterranean Sea.

The importance of the present study relates to the fact that most of the current knowledge on *T. lyra* needs to be updated, and there is little to no information about the populations of the species in Portuguese waters. Moreover, for a sustainable exploration, management and valorisation of this species it is important to investigate the age and growth, the reproduction as well as the chemical composition of the fish, which are addressed in the present work.

1.4. Main objectives

The objectives of the present study were to evaluate the age and growth, study the reproduction, and analyse the chemical composition of *T. lyra*. Regarding age and growth, reading protocols were established in whole otoliths (comparison of different reading zones, and burned versus not burned otoliths), age estimation was performed, age-length key was constructed, the von Bertalanffy growth model was adjusted to the data and growth parameters were estimated, and length-weight relationship was determined. Regarding reproduction, this study aimed to characterize the reproductive strategy of the species including definition and duration of the spawning season and analysis of the gonadosomatic (GSI) and hepatosomatic (HSI) indexes and Fulton's condition factor (K), characterize the reproductive strategy, including ovary organization, gender system, fertilization type and spawning pattern, and identify the species fecundity type. Finally, the chemical composition of *T. lyra* was determined in terms of ash content, moisture, total fat, protein content and profile of fatty acids.

The present work is included in a MAR 2020 project entitled "VALOREJET – Aproveitamento de espécies rejeitadas e de baixo valor comercial: valorização de novos produtos com recurso a metodologias inovadoras" which aims to evaluate the potential use of fish species with no or low commercial value and to develop new products from these species, using innovative and improved techniques and processes.

2. Material and methods

2.1. Sampling

A total of 492 *T. lyra* specimens were collected between May 2018 and May 2019 (excluding June, July and August) from commercial fishing vessels operating off mainland Portugal (Peniche, West coast) using trawls, trammel nets, traps and pots. A sub-sample of approximately 30 individuals from different length-classes, was selected and transported monthly to the Fisheries Biology laboratory in the Faculdade de Ciências da Universidade de Lisboa, for later analysis. During the spawning season samples were collected every two weeks.

Once in the laboratory, samples were processed in fresh, and total length (TL, to the nearest 0.1 cm) and total weight (TW, to the nearest 0.01 g) of each fish were measured, using an ichthyometer (Fig. 2.1) and a digital scale, respectively. The abdominal cavity of individuals was exposed, and the gonads and liver separated from the rest of the organs (Fig. 2.2B) and weighted (to the nearest 0.01 g). The weight of the gonads and liver is represented by GW and LW, respectively.

Sex was identified by macroscopic examination of the gonads. Ovaries are usually tubular, red/pink, and granular while the testes are flat, white-grey/brown (Holden and Raitt, 1974). The macroscopic determination of phases in the reproductive cycle was based on general features, namely shape, colour, size, texture, consistency, vascularization, presence/absence of visible oocytes (females), efferent duct visible (males), release of sperm when touching (males), and following the general terminology proposed by Brown-Peterson et al. (2011) and based on the criteria established by Murua et al. (2003) for females. However, as it is recommended the use of histology to validate the macroscopic classification and to describe gonad developmental for a thorough fish reproduction study (Alonso-Fernández et al., 2008; Domínguez-Petit et al., 2017), histological procedures were taken to confirm the phase of maturity of all fish sampled.

The remaining contents from the abdominal cavity were removed and the eviscerated weight (EW, to the nearest 0.01 g) of each fish registered. Immediately after sampling, gonads were preserved in 4% buffered formalin and stored in labelled plastic tubes for later processing and histological analysis.

Sagitta otoliths (left and right) were removed from the head of the fish through a ventral cranium section (Fig. 2.2A), as described in Panfili (2002). After removal, otoliths were

washed with tap water to remove the *sacculus*, cleaned with absorbent paper, air dried and stored in labelled plastic tubes for later analysis.

Differences between TL of males and females were tested with the Student's *t*-test (Zar, 1999).

Fig. 2.1. Specimen of *Trigla lyra*.

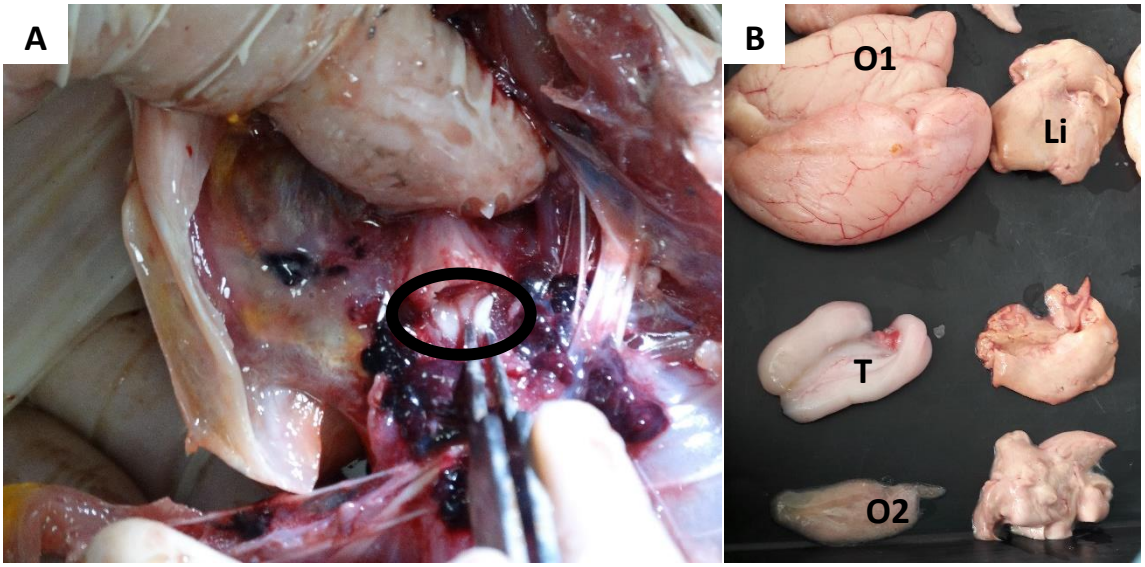

Fig. 2.2. (A) Removal of *sagitta* otoliths (black ellipse) from the head of *Trigla lyra*, through a ventral cranium section. (B) Separation of gonads and liver of *T. lyra*. O1, ovaries in actively spawning phase; T, testes; O2, ovaries in regressing phase; Li, liver.

2.2. Age and growth

2.2.1. Otolith morphology

Description of the morphology of *T. lyra sagitta* otoliths was done based on the nomenclature of Kalish et al. (1995), Assis (2000) and Wright et al. (2002).

2.2.2. Age estimation methodology and validation

Before starting age estimation of *T. lyra*, age reading protocols were established by comparing burned with unburned otoliths (Fig. 2.3B) and testing different reading zones in the otolith (posterior, anterior, dorsal, ventral) (Fig. 2.3A). A sample of 31 pairs of *sagitta* otoliths by length classes of 1 cm (between 11.2 and 41.4 cm TL) and from both sexes (whenever possible) was chosen. The left otolith was burned in the drying oven at 200ºC during 25 min. Although previous studies suggested the use of 450 ºC for the process (Papaconstantinou, 1981; Papaconstantinou et al., 1992) the temperature of 200 ºC was chosen due to equipment constraints. Burned otoliths were compared with unburned otoliths, and the latter showed a better differentiation and visibility of growth increments. The posterior zone of the otolith presented a larger radius as well as a better differentiation and individualization of the growth increments (Fig. 2.3A). Given this, the posterior zone of unburned otoliths was the selected for age reading.

To establish a reading and interpretation pattern and to assure consistency among readings, a representative subsample of 75 right *sagitta* otoliths covering all length classes was read by three readers. The average percent error (APE) (Beamish and Fournier,1981), the coefficient of variation (CV) (Chang, 1982) and the index of precision (D) (Chang, 1982) were determined to compare readings between the readers and were determined as follows:

$$\mathrm{APE} = 100 \times \frac{1}{R} \sum_{i=1}^{R} \frac{| Xij - Xj |}{Xj}$$

$$\mathrm{CV} = 100 \times \frac{\sqrt{\sum_{i=1}^{R} \frac{(Xij - Xj)^2}{R-1}}}{Xj}$$

$$D = \frac{CV}{\sqrt{R}}$$

Where, Xij is the age determination of the *j*th fish, Xj is the mean age of the *j*th fish, and R is the number of times each fish was aged.

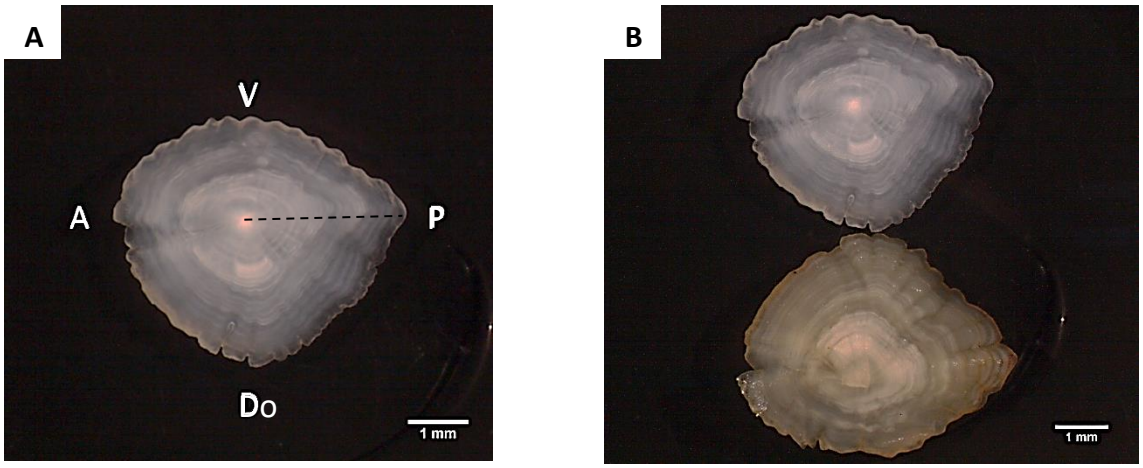

Fig. 2.3. (A) External surface of the right *sagitta* otolith of an individual of *Trigla lyra* with 38.2 cm TL. Dashed line represents the reading axis. V, ventral edge; Do, dorsal edge; A, anterior region; P, posterior region. (B) Pair of *sagitta* otoliths of the same individual. Right otolith is on the top and left otolith, which was burned in the drying oven at 200 ºC, is at the bottom. Scale bar = 1 mm.

Age bias plots were used to investigate deviations of the age readings among readers from the 1:1 equivalence line (Campana et al., 1995).

After assuring consistency among readings, a subsample of 12 right otoliths per length class including males and females was selected and read by one reader. The right otolith was immersed in water and read on a stereomicroscope under reflected light with a 18x magnification and against a black background. The translucent annual growth increments (also known as *annuli*) were counted with the *sulcus acusticus* placed downwards, on the posterior zone of the otolith, from the nucleus to the edge of the otolith. The distances from the nucleus to each successive translucent increment (nucleus-to-increment distances), as well as distances from the nucleus to the edge of the otolith were measured using a calibrated micrometer eyepiece.

The marginal increment ratio (MIR) (Samamé, 1977) was determined for each month of sampling using the nucleus-to-increment distances and used for validating the annual increment periodicity. The edge of the otoliths was classified as translucent (dark

increment) or opaque (light increment). Mean MIR and standard error, and edge type were plotted by month to assess if there were any annual trends in the formation of growth *annuli*.

2.2.3. Length-weight relationship

Length-weight relationship is commonly used in fishery biology as it allows to obtain some biological information on the target species. For example, if the length of a fish is known it may be useful to determine the weight correspondent to that length, which may provide information on general condition of the individual, overall growth and gonad development (Le Cren, 1951). The relationship between TL and EW was calculated using a power function:

$$\mathrm{EW} = a\mathrm{TL}^{b}$$

where *a* is the intercept and *b* is the slope (Le Cren, 1951; Ricker, 1973).

The Student's *t*-test was performed to compare the slopes of the function between males and females and to test the allometry in growth (Zar, 1999).

2.2.4. Growth model

The Mann-Whitney test was used to verify if there were differences in growth by sex, comparing length-at-age data between males and females (Zar, 1999), given the lower representativeness of ages in males comparing with females. As significant differences were not found ($p > 0.05$), a population age-length key was compiled (see Results section 3.2.2).

To estimate growth of the piper gurnard the von Bertalanffy growth model was used (von Bertalanffy, 1938), which is described by the equation:

$$\mathrm{Lt} = \mathrm{L}\infty\,[1 - \mathrm{e} - \mathrm{k}\,(\mathrm{t} - \mathrm{t0})]$$

where L_∞ is the mean asymptotic length, k is the growth parameter, and t_0 is the theoretical age at which the length of the fish is zero.

Since there was an under representativeness of individuals smaller than 23 cm in the sampling, three methods were used to estimate von Bertalanffy growth parameters and find the best adjustment model to describe *T. lyra* growth: whole otolith reading, back-calculation (Francis, 1990; Jones, 2000; Wilson et al., 2009) and a combination of the two methodologies (Gordo et al., 2016). For whole otolith approach, sampled individuals

between 12.5 cm and 41 cm TL (1-10 years) were used. Back-calculation is used to reconstruct data for growth analysis, as it allows inferring the length of a fish at younger ages that may not be represented in the sampling, thereby increasing the number of length-at-age data to be used in fitting a growth model to the data. A prerequisite for applying this technique is the existence of a relationship between body-length and otolith radius (OR) (Francis, 1990; Jones, 2000), which was determined for *T. lyra*, through the following power function:

$$\mathrm{EW} = a\mathrm{OR}^{b}$$

where *a* is the intercept and *b* is the slope. Then, age-length data was reconstructed using this function.

The combined methodology consisted in using information provided by back-calculation on the ages lower than two years and information provided by whole otolith readings on the ages from 3-10 years.

The Akaike's information criterion corrected for small samples (c-AIC; Shono, 2000) was determined to evaluate which was the best approach to estimate the von Bertalanffy growth parameters.

2.3. Reproduction

2.3.1. Sex ratio

Sex ratio of sampled individuals was determined for each month of sampling and significant differences from 1/1 ratio (number of females/number of males) were evaluated with Pearson's Chi-squared test (Zar, 1999).

2.3.2. Structure of the gonads

Histological processing of the gonads was performed for 345 individuals - 284 females, 60 males, and 1 immature – following the protocol described in Appendix I. To characterize oocytes in each stage of oogenesis, the histological sections were analysed based on information provided by Wallace and Selman (1981) and Lowerre-Barbieri et al. (2011a). Stages of oogenesis were classified as follows: primary growth (PG), cortical alveolar (CA), primary and secondary vitellogenic (<Vtg3), tertiary vitellogenic (Vtg3), oocyte maturation (OM) and hydrated (H). Oocyte maturation includes four stages of oogenesis, which are germinal vesicle migration (GVM), yolk coalescent (YC), germinal

vesicle breakdown (GMVB) and H. Since it was difficult to distinguish in the histological sections some advanced stages of oogenesis, particularly the GVM and GVMB, it was decided to use the designation of oocyte maturation (OM) for GVM, YC and GVMB oocytes, and hydrated (H) separately from OM.

To characterize each cellular stage of spermatogenesis, the obtained histological sections of males were analysed following Grier (1981): spermatogonia (Sg), spermatocytes (Sc), spermatids (St) and spermatozoids (Sz).

Digitized images of the histological sections were obtained using a visual image analysis system (Leica Application System V4.12). Approximately 100 cells in each development stage and with visible nucleus were measured for their maximum and minimum diameter which were averaged afterwards, to minimize the error from the loss of spherical shape due to histological processing. Female and male cells were chosen from individuals of all maturity phases and analysed using the software package ImageJ (https://imagej.nih.gov/ij/) with the ObjectJ plugin (https://sils.fnwi.uva.nl/bcb/objectj/).

To measure the diameter of hydrated oocytes, three females in actively spawning phase (AS) with hydrated oocytes were chosen and sub-samples of the ovaries were taken and placed on a watch glass dish. Digital images were obtained under the stereomicroscope (Fig. 2.4) and were analysed using the software Image J.

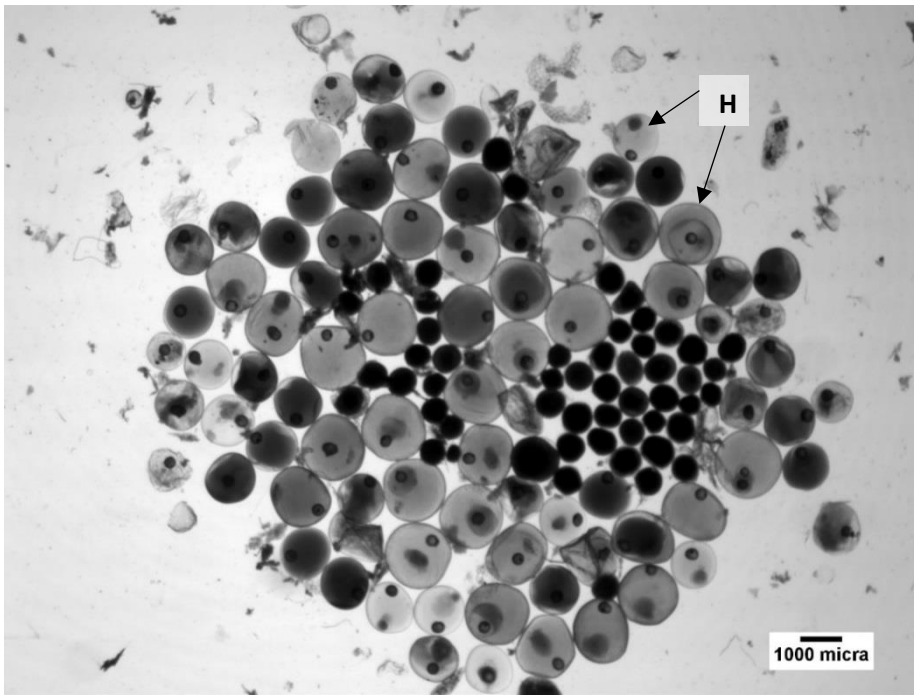

Fig. 2.4. Digital image representing oocytes of an ovary of an actively spawning female of *Trigla lyra*, obtained under a stereomicroscope. H, hydrated oocyte.

2.3.3. Sexual cycle and spawning season characterization

Gonads were histologically classified according to the maturity phase of the reproductive cycle, based on the universal terminology proposed by Brown-Peterson et al. (2011): immature (I), developing (De), spawning capable (SC) [and the actively spawning subphase (AS), in females], regressing (RG) and regenerating (RN). The attribution of the maturity phase of a gonad considered the development stage of the most advanced cellular type present.

The annual sexual cycle of *T. lyra* was studied based on the monthly frequency of the maturity phases for both genders throughout the year, which was further corroborated with the monthly progress of the gonadosomatic (GSI = 100× GW/EW) and hepatosomatic indexes (HSI = 100 × LW/EW). The Fulton's condition factor (K = 100 × EW/TL^3), which provides information on fish condition, was also determined for both sexes along the annual cycle. Significant differences in the indices over the year and by maturity phase were investigated using the non-parametric Kruskal-Wallis rank sum test and post-hoc tests according to Nemenyi for pairwise multiple comparisons of the ranked data (Zar, 1999).

The spawning season of *T. lyra* was defined based on the period between the first month when 50 % of females were in pre-spawning condition (*i.e.*, presence of oocytes in tertiary vitellogenesis with no signs of hydration and/or previous spawning), and the month when 50 % of females were in postspawning condition (spent and recovering). The peak of spawning corresponded to the month with highest percentage of females in actively spawning phase (Murua et al., 2003; Lowerre-Barbieri et al., 2011b).

2.3.4. Fecundity

Before fecundity studies, it is important to assess the homogeneity of the distribution of oocytes in the ovary to guarantee the representativeness of the sub-sample to be used Murua et al. (2003). A uniform distribution of oocytes in the ovary and between the pair of ovaries needs to be warranted (Ganias et al., 2014). Therefore, to check for differences in the distribution of oocytes in the ovary, samples from posterior, medium and anterior regions of the right ovary lobe of three SC females were collected. To check for differences in the distribution of oocytes between the two lobes of the ovary, samples from the medium region of the right and left ovary lobes of the same females used for the previous analysis were collected. The beta regression model was used to compare the

diameter-specific frequency of oocytes above 150 µm between zones and lobes in the ovary.

Based on the studies of Hunter et al. (1992), Greer Walker et al. (1994), Murua and Saborido-Rey (2003), and Ganias et al. (2014), four criteria or lines of evidence were used to assess whether the fecundity type of *T. lyra* was determinate or indeterminate: (1) the phase-specific and monthly-specific variation of oocyte size-frequency distribution during the reproductive cycle; (2) the variation of the number of advanced yolked oocytes in the ovary during the spawning season; (3) the evolution of the mean diameter of advanced vitellogenic oocytes over the spawning season; and (4) the occurrence of atresia during the spawning season.

The first three criteria were investigated using the gravimetric method as suggested by Ganias et al. (2014). Thus, the number and mean diameter of oocytes from CA state onwards was counted in ovary subsamples and the total number of oocytes in the gonad was subsequently calculated by multiplying the sum of the number of oocytes in the subsamples divided by the sum of the subsample weights by the weight of the gonad. Three subsamples between 0.01 g and 0.03g were taken from the middle part of the right ovary lobe of each female, weighted (to the nearest 0.01 g) and flushed with tap water into a 125 µm mesh sieve, which size was dependent on the diameter of the cortical alveolar oocytes measured in histological sections which proved to be higher than 125 µm (chapter 3, Table 3.5). Afterwards, samples were placed on a watch glass dish and oocytes were separated from each other and from connective tissue with needles and forceps, when required. Digital images were obtained under a stereomicroscope (Fig. 2.5A) and oocytes were automatically measured and counted using ImageJ software with the ObjectJ plugin (https://sils.fnwi.uva.nl/bcb/objectj/) (Fig. 2.5B). Manual correction was applied, when needed, in each processed image to include the oocytes not automatically detected and eliminate those incorrectly marked.

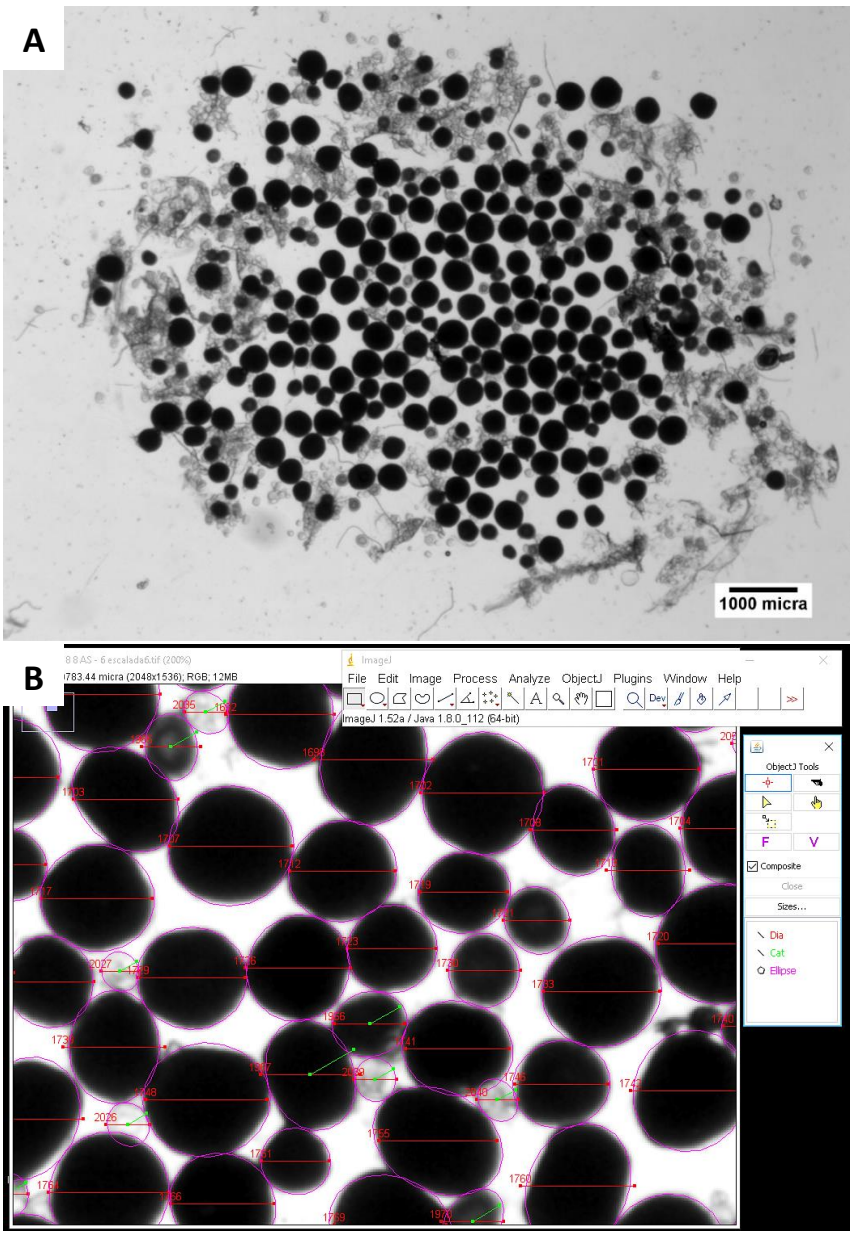

Fig. 2.5. (A) Digital image representing oocytes of a sub-sample of an ovary of a spawning capable female of *Trigla lyra*, obtained under a stereomicroscope; (B) Oocyte analysis using ImageJ software with the ObjectJ plugin (https://sils.fnwi.uva.nl/bcb/objectj/). The automatic analysis surrounds the oocytes with the best-fitting ellipse and constructs a horizontal pink line inside the oocytes which represents the diameter of the oocyte. Some oocytes needed to be manually measured, getting a green line inside.

To study the phase-specific variation of oocyte size-frequency distribution (first criteria), five females per maturity phase (from De to RG) were chosen. To assess the monthly-specific variation of oocyte size-frequency distribution during the spawning season (first criteria) and to analyse the variation of the number (second criteria) and the evolution of the mean diameter (third criteria) of advanced yolked oocytes in the ovary during the

spawning season, five females in SC phase from each date of sampling during spawning season were chosen. Differences among sampling dates were analysed with the non-parametric Kruskal-Wallis test (Zar, 1999) for the second and third lines of evidence.

To investigate the fourth line of evidence, the percentage of ovaries showing atresia by month was determined through the histological analysis of all females sampled in the spawning season.

2.4. Chemical composition of the muscle

Determination of relative moisture, ash content, protein content, total fat content and profile of fatty acids was done for *T. lyra*, using fish caught during January, March and May 2019. Differences in the chemical composition over the months were investigated with non-parametric Kruskal-Wallis rank sum test and post-hoc tests according to Nemenyi for pairwise multiple comparisons of the ranked data (Zar, 1999). A sample of fresh individuals from different lengths was chosen and scales, head, fins and guts of each fish were removed. The edible part of the fish was used for chemical composition analysis. Portions of the edible part were weighted in 50 ml falcons, stored at -80 ºC and lyophilized, except for moisture and ash determination, where fresh samples were used. Before chemical analysis, lyophilized samples were homogenized in a mincing machine.

2.4.1. Relative moisture

Relative moisture was determined based on the method described in NP 2282 (Portuguese Institute of Quality, 1991).

Initially, three crucibles (three replicates) were put in the drying oven to dry and remove any traces of moisture that could be present. After 15 min, the crucibles were weighted (to the nearest 0.01 g) (m1). Then, approximately 10 g of fresh sample of muscle in each crucible were weighted (to the nearest 0.01 g) (m2). After this, the samples were kept in the drying oven at 105 ºC for 3 hours. After this period, the samples were kept in the desiccator for cooling, and then weighted. The process of weighing was repeated until the samples reached a stable weight.

The relative moisture of *T. lyra* was determined according to the following equation:

$$\%\ \text{Moisture in wet base} = \frac{\text{m2} - \text{m3}}{m2 - m1} \times 100$$

where m1 is the weight of the crucible, m2 is the weight of the crucible plus the fresh sample, and m3 is the average weight of the crucible plus the dry sample. At the end, the average of the % moisture of the three replicates was determined.

2.4.2. Ash content

Determination of ash content, constituting the mineral residuals obtained by incineration, was based on NP 2032 (Portuguese Institute of Quality, 1988).

The dehydrated samples (three replicates) that were obtained in relative moisture determination, were used for ash determination after constant weight was obtained. Then, samples were heated during 30 min, carbonized in Bunsen burner and then heated at 525-550 ºC for 4 hours, transforming them in ash. After this, the samples were put in the desiccator and weighted.

The content in ash of *T. lyra* was determined according to the following equation:

$$\text{ash content (\%)} = \frac{(\text{m3} - \text{m1})}{(\text{m2} - \text{m1})} \text{x } 100$$

where m1 is the weight of the crucible, m2 is the weight of the crucible plus the dehydrated sample, and m3 is the weight of the crucible plus ash. At the end, the average of the ash content of the three replicates was determined.

2.4.3. Protein content

To determine the protein content of *T. lyra*, the procedures followed the Kjeldahl method (quantification of total nitrogen) (Kjeldahl, 1883). This method consists in the acid digestion, distillation and lastly the titration of the sample.

First, 2 g of lyophilized sample were weighted (to the nearest 0.01 g) in a Kjeldahl tube (three replicates), adding 2 pellets of Kjeldahl catalyst and 25 ml of 98% sulphuric acid (H_2SO_4), and digesting it in the Kjeldahl digestor with two cycles at high temperatures, for 2 hours. After the digestion of the sample, it was distilled with 40% sodium hydroxide solution to an Erlenmeyer flask with 30 ml of 40% boric acid solution. The obtained distilled was titrated with a pattern solution of chloridric acid. The procedure mentioned previously was repeated for two Kjeldahl tubes containing 2 pellets of Kjeldahl catalyst and 25 ml of 98% sulphuric acid (blank).

The crude protein content was determined according to the following equation:

$$\text{Protein content} = \frac{1{,}4007 \text{ x } (Va - Vb) \text{x } N}{m} \text{ x } 6{,}25 \text{ (g of protein/100g of sample)}$$

where Va is the volume of titrant used, Vb is the volume of titrant used in the blank essay, N is the concentration of chloridric acid used, and m is the weight of the sample.

2.4.4. Total fat

Total fat was determined following the Folch method (Folch et al., 1957). The method consists in weighting approximately 1 g of lyophilized sample (to the nearest 0.01 g) to a falcon 50 ml, adding 0.8 ml of water, 5 ml of Folch reagent, and putting in the vortex for 1 min. Then, 5 ml of Folch reagent was added, and it was put in the vortex for 5 min. After this, a 0.8 % sodium chloride solution was added, and the mixture was put in the vortex for 2 min and then centrifuged at 6000 rpm, at 4ºC for 10 min. The centrifuged was filtered in column (with hydrophobic cotton and anhydrous sodium sulphate) and then weighted. The chloroform of the centrifuged was removed and the mixture filtered again. After this, 5 ml of chloroform ($CHCl_3$) was added to the mixture which was centrifuged again. After filtering the chloroform, the solvent was evaporated at 40 ºC in a glass recipient. Finally, the obtained product was dried in the drying oven for 3 hours, and then weighted until reaching a stable weight.

The total free fat content was determined using the following equation:

$$\text{Total free fat (\%)} = \left(\frac{Wf - Wi}{Ws}\right) \times 100 \text{ (g of fat/100g of lyophilized sample)}$$

Where, Wi is the weight of the glass recipient, Wf is the average weight of the dry sample plus the glass recipient, and Ws is the initial weight of the sample.

2.4.5. Profile of fatty acids

A fatty acid methyl ester mix was used as gas chromatography standards (SupelcoTM 37 Component FAME Mix, Sigma-Aldrich). All solvents used for sample preparation were of analytical grade and the solvents used for gas chromatography analysis were of HPLC grade. Profile of fatty acids was determined by direct acid-catalysed transmethylation of the lyophilized fish material following Fernández et al. (2015). For this purpose, 50 mg of lyophilized sample was weighted (to the nearest 0.0001 mg) in a vial (three replicates), and 2 ml of a 2% (v/v) sulphuric acid (H_2SO_4) solution in dry methanol was added. The mixture was heated for 2 hours at 80 ºC with continuous stirring under a nitrogen

atmosphere. After cooling to room temperature, 1 ml of MiliQ water and 2 ml of n-hexane were added and each vial was put in the vortex for 1 min and then centrifuged at 1000 rpm for 5 min. After this, 1 ml of the upper n-hexane phase containing the FAMEs (fatty acid methyl esters) was recovered and transferred to gas chromatography vials of 500 µL. The upper organic phase was recovered and analysed by gas chromatography (GC) in Gas Chromatography – Flame Ionization Detector (GC-FID) (Fig. 2.9). A Finnigan Ultra Trace gas chromatograph equipped with a Thermo TR-FAME capillary column (60 m × 0.25 mm ID, 0.25 µm film thickness), an auto sampler AS 3000 from Thermo Electron Corporation and a flame ionization detector (FID) were used to analyse the fatty acids methyl esters. The injector (operating in splitless mode) and the detector temperatures were set at 250 and 280 °C, respectively. The column temperature was initially set at 75 °C for 1 min, then raised at 5 °C min^{-1} to 170 °C and held for 10 min followed by an increase at 5 °C min^{-1} to 190 °C and maintained for 10 min, and finally raised to 240 ºC at 2 ºC min^{-1} and held for 10 min. Helium was used as carrier gas at a flow rate of 1.5 mL min^{-1}. Air and hydrogen were supplied to the detector at flow rates of 350 and 35 mL min^{-1}, respectively. Significant differences in fatty acid composition between months of sampling were investigated with one-way ANOVA post hoc tests and pairwise multiple comparisons were conducted with the Tukey's honestly significant difference test (Zar, 1999).

3. Results

3.1. Sampling

A total of 492 individuals (381 females, 77.4 %, 110 males, 22.4 %, and 1 immature, 0.2 %) with lengths ranging from 12.5 cm to 45.1 cm were collected between May 2018 to May 2019. The distribution of individuals by length class is represented in Figure 3.1, with the highest number of females occurring in the length class of 29-30 cm (n = 53) and the highest number of males occurring in the length class of 27-28 cm (n = 20). Most of the individuals sampled had more than 23 cm of TL, which highlights the lack of smaller individuals in the sample. Furthermore, the results showed differences between both sexes in length-frequency distributions, with females reaching higher lengths than males. The mean TL for females was significantly higher than the mean TL for males (t-test = 2.35; $p < 0.05$). Females ranged from 23.5 cm to 45.1 cm TL while males ranged from 25.8 cm to 41.0 cm TL.

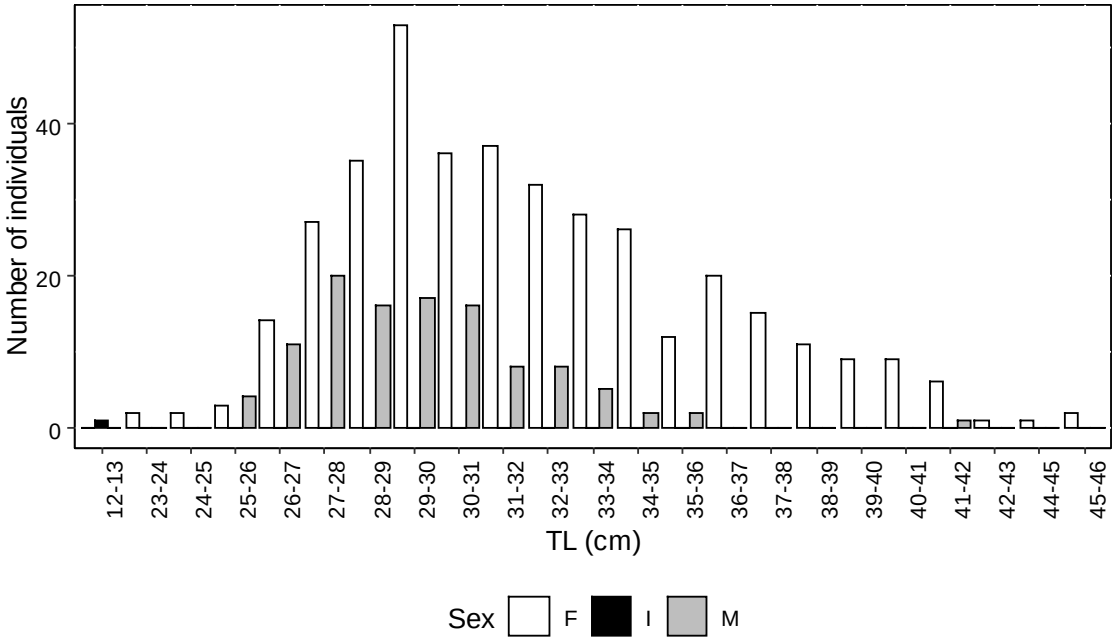

Fig. 3.1. Length-frequency distribution of *Trigla lyra*. White bars correspond to females, grey bars correspond to males and black bars correspond to immature. Classes of 1 cm interval were used.

3.2. Age and Growth

3.2.1. Otolith morphology

The *sagitta* otoliths of *T. lyra* presented a general shape that could vary between more triangular or more oval. Otolith margin was wavy in dorsal and ventral edges, as well as in posterior and anterior regions. In general, otoliths presented a steeper curvature in the dorsal edge compared to the ventral edge, a larger length than height, a median apex in the dorsal edge, a rounded anterior region and a pointed posterior region. Furthermore, some common structures in the otoliths were identified, namely the *rostrum*, the *antirostrum* and the *sulcus acusticus* (Fig. 3.2). *Rostrum* consisted in a protuberance on the most anterior edge of the otolith, while *antirostrum* was also a protuberance but was located dorsally to the *rostrum*. *Sulcus acusticus* consisted in a groove with variable depth depending on the individual, which divides the otolith longitudinally into a lower and an upper part.

A regular pattern of deposition of annual growth increments (*annuli*) in the otolith was visible, with alternate opaque and translucent concentric increments deposited around an opaque nucleus. Increments were wider closer to the nucleus and thinner towards the edge of the otolith.

In general, the size of the otolith increased with increasing length of the individual. However, this increase was not very pronounced and did not apply to all individuals, as there were many larger individuals with small otoliths, which is denoted by the relationship between fish body length and otolith radius (Fig. 3.6). Furthermore, the presence of some discontinuities in the otolith, for example, false increments, have been identified in some otoliths.

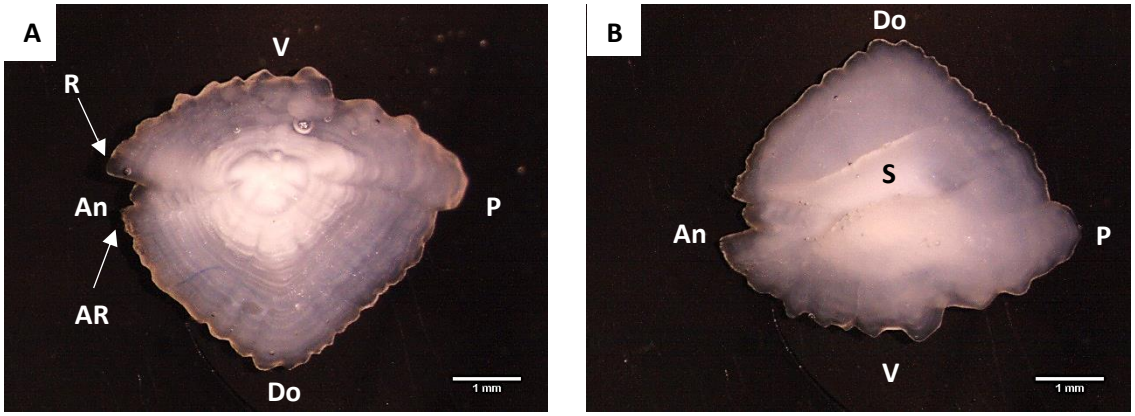

Fig. 3.2. External (A) and internal (B) faces of the right *sagitta* otolith of an individual of *Trigla lyra* with 37.9 cm TL. V, ventral edge; Do, dorsal edge; An, anterior region; P, posterior region; AR, *antirostrum*; R, *rostrum*; S, *sulcus acusticus*. Scale bar = 1 mm.

3.2.2. Age estimation and validation

To establish a reading pattern, 75 right *sagitta* otoliths of *T. lyra* were analysed by three readers. The estimates of average percent error (APE), coefficient of variation (CV) and index of precision (D) for age readings between readers are presented in Table 3.1. The lowest indices values (APE, CV and D) were obtained between readers 1 and 2, while the highest values were obtained between readers 2 and 3. Overall, the lowest precision was achieved between readers 2 and 3 (CV = 11.493 %; APE = 8.127 %; D = 8.127 %) and the highest between readers 1 and 2 (CV = 9.514 %; APE = 6.727 %; D = 6.727 %).

A good total agreement over 80% between all readers was achieved, with higher values observed between readers 2 and 3. Nevertheless, age bias plots (Fig. 3.3) comparing age estimation between readers showed some deviation from the 1:1 equivalence line, indicating some disagreement in age assignment between readers, particularly for ages greater than 5/6 years.

Table 3.1. Indices of precision for age readings of *Trigla lyra*, between readers.

Index	Comparison		
	Readers 1 and 2	Readers 1 and 3	Readers 2 and 3
APE (%)	6.727	7.235	8.127
CV (%)	9.514	10.232	11.493
D (%)	6.727	7.235	8.127
Total agreement (%)	85.333	80.000	87.324

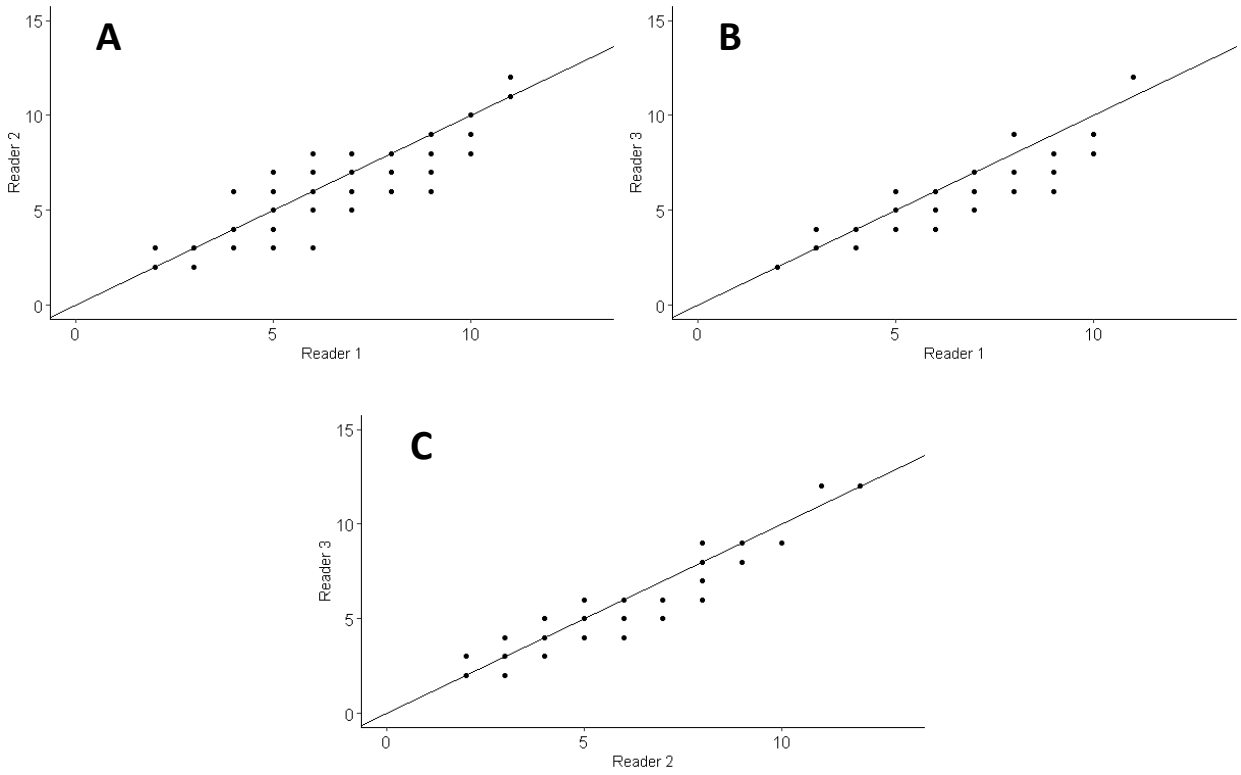

Fig. 3.3. Age bias plots for the readings comparisons between readers for *Trigla lyra*: (A) readers 1 and 2, (B) readers 1 and 3, (C) readers 2 and 3.

After validating age readings between readers, a total of 275 whole right *sagitta* otoliths were analysed from individuals with TL ranging between 12.5 cm and 45.1 cm. Age-length key for the species is represented in Table 3.2. Females ranged from 23.5 cm to 45.1 cm and were aged from 2 to 12 years, males ranged from 25.8 cm to 41.0 cm and were aged from 2 to 10 years, and the immature individual had 12.5 cm of TL and 1 year of age. The maximum age attained by *T. lyra* was 12 years, with 45.1 cm of TL.

Table 3.2. Age-length key for *Trigla lyra*, for the period between May 2018 and May 2019. N, number of fishes; TL mean, mean total length; SD, standard deviation.

TL (cm)	**Age (yr)**												**Total**
	1	2	3	4	5	6	7	8	9	10	11	12	
12-13	1												1
23-24		1											1
24-25		1	1										2
25-26			1										1
26-27		4	14										18
27-28		2	12	9	1								24
28-29		2	13	7	6	1							29
29-30			1	13	9								23
30-31			2	10	11								23
31-32			1	8	9	1	1						20
32-33				7	6	6							19
33-34				2	8	6	1						17
34-35					3	9	2						14
35-36					3	5	5						13
36-37						11	5	3					19
37-38						4	7	3					14
38-39						1	4	4	2				11
39-40								4	2				6
40-41							1	5	2	1			9
41-42									3	4			7
42-43									1				1
44-45											1		1
45-46												2	2
N	1	10	45	56	56	44	26	19	10	5	1	2	275
TL mean	12,5	26,7	27,5	30,0	31,2	34,8	36,5	38,6	40,3	40,9	44,4	45,1	
SD		1,5	1,4	1,7	2,0	2,0	1,7	1,4	1,3	0,6	-	0,0	

The evolution of marginal increment ratio and proportion of opaque and translucent otolith edges throughout the months of sampling are represented in Figure 3.4. MIR showed a similar evolution to otolith edge. The highest value of MIR occurred in May 2019, as well as the highest proportion of opaque edges. There was a decreasing trend of MIR from September 2018 to December 2018, and then an increase until May 2019. Translucent edges were more frequent than opaque edges during the months of sampling, although it is possible to see that there was a higher proportion of translucent edges in the months of winter and a higher proportion of opaque edges in September 2018 and May 2019, which are after and before the summer period.

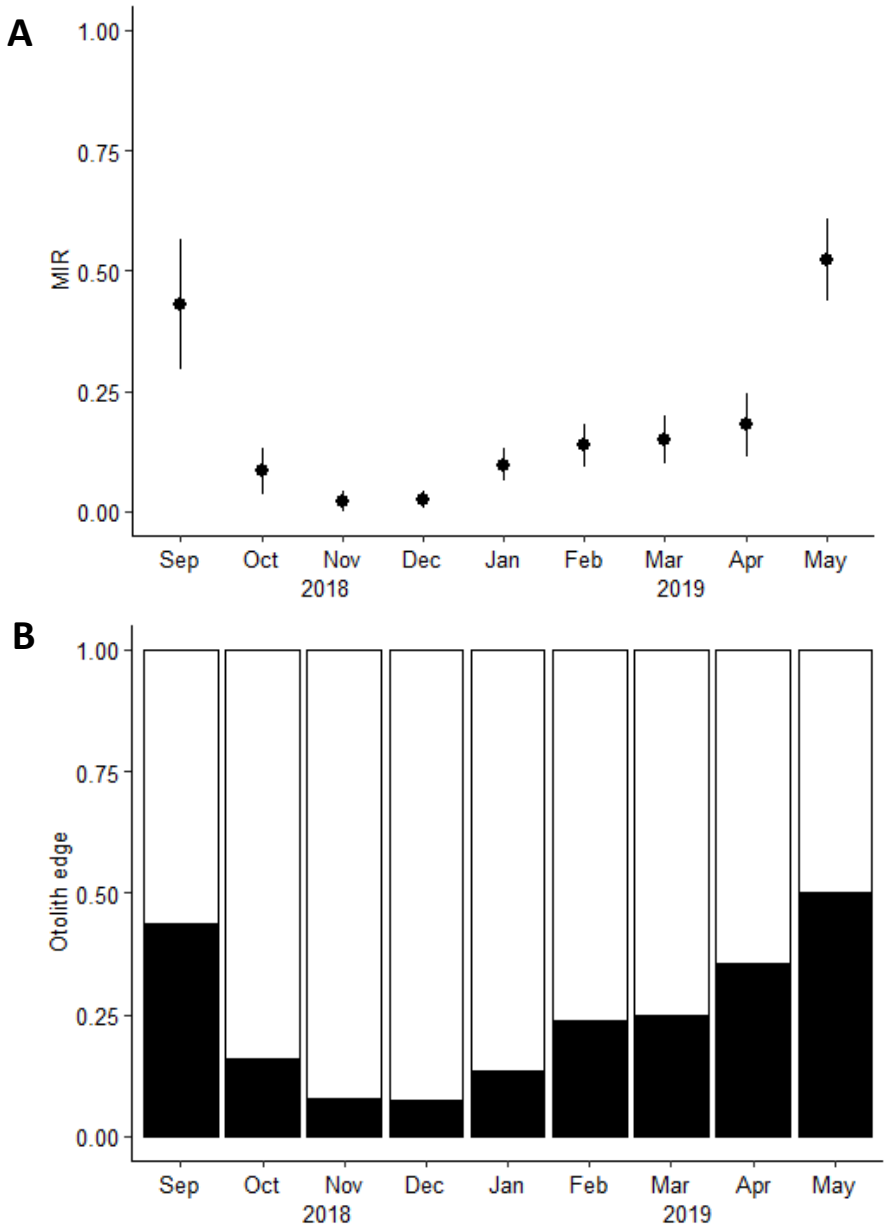

Fig. 3.4. (A) Evolution of marginal increment ratio (MIR) in whole otoliths of *Trigla lyra*. Standard error bars are represented. (B) Evolution of the proportion of translucent and opaque otolith edges in whole otoliths of *T. lyra* along the months of sampling. Black bars represent opaque edges and white bars represent translucent edges.

3.2.3. Length-weight relationship

Length-weight relationship was determined for a total of 492 individuals (Fig. 3.5). The equations that express the length-weight relationship for piper gurnard, *T. lyra*, were:

$EW = 0.0072054TL^{3.0252615}$ ($R^2 = 0.9561$) for females

$EW = 0.005664TL^{3.085932}$ ($R^2 = 0.9351$) for males

$EW = 0.0064269TL^{3.0563468}$ ($R^2 = 0.9582$) for the entire sample

There were no significant differences between the growth of males and females (paired t-test: t-test = 0.915, $p > 0.05$). The results indicated that *b* was not significantly different from 3 for both males and females (paired t-test, females: t-test = 0.7028994, $p > 0.05$; males: t-test = 1.54, $p > 0.05$).

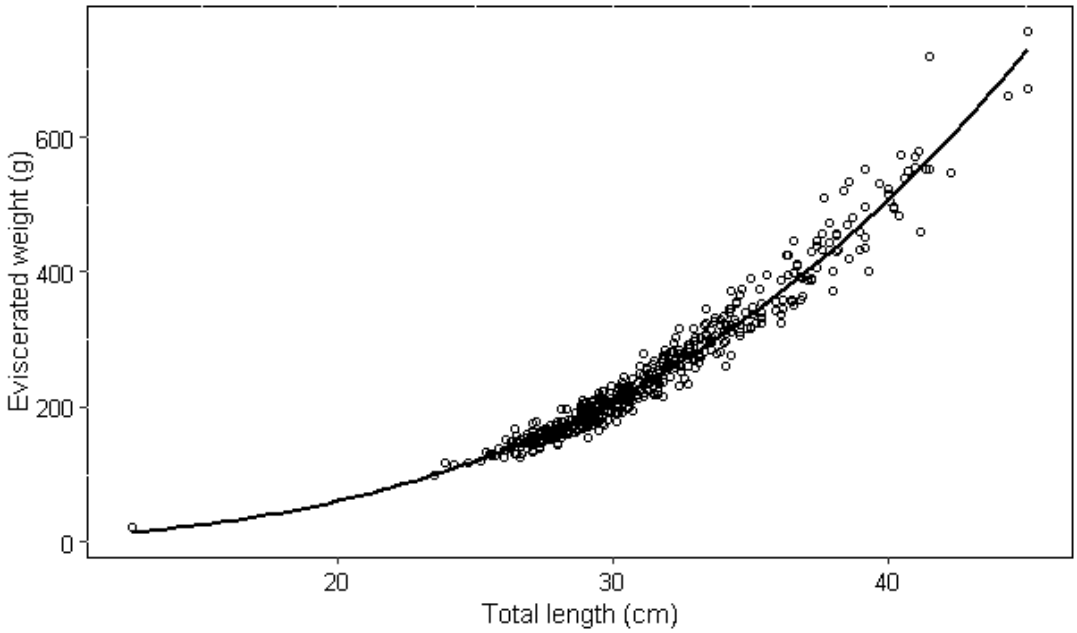

Fig. 3.5. Length-weight relationship for all sampled individuals of *Trigla lyra*.

3.2.4. Growth model

Due to the under representativeness of smaller individuals in the sample and due to the lower representativeness of males, differences in the mean length by length class at age between females and males were checked, considering only length classes with more than 10 individuals. There were no significant differences in the mean length per length class at age between sexes ($p > 0.05$), and therefore the estimation of von Bertalanffy growth model parameters was done for the entire sample.

For the back-calculation method, the relationship between body length (TL) and otolith radius (OR) was determined for 275 individuals and is represented in Figure 3.6 and expressed by the following equation:

$TL = 10.449\ OR^{1.1062}$; $R^2 = 0.6731$.

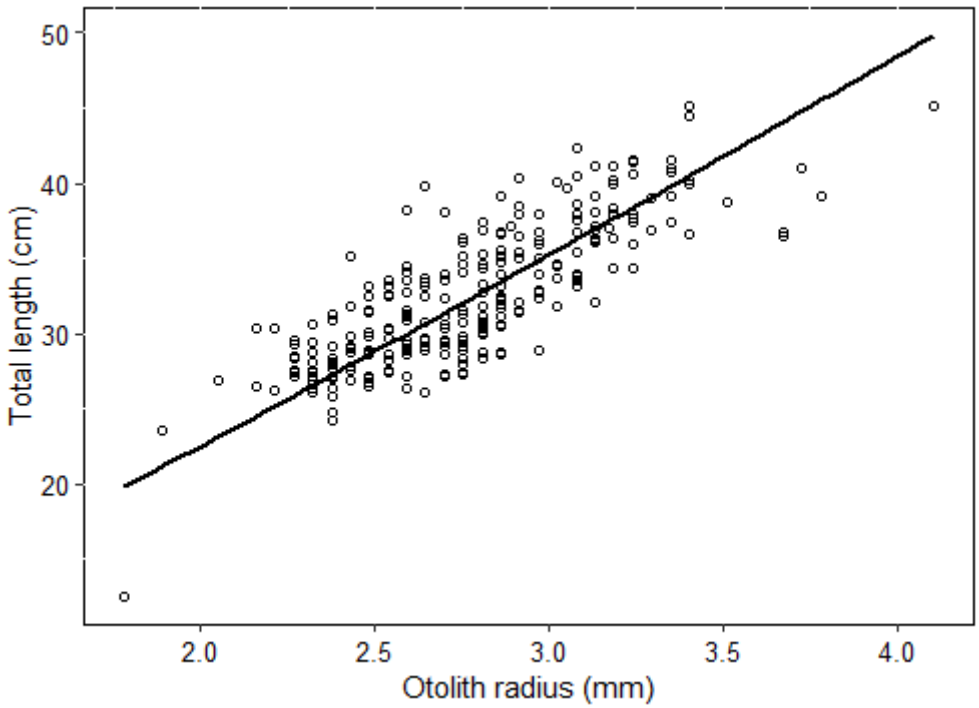

Fig. 3.6. Relationship between fish body length and otolith radius in *Trigla lyra*.

The estimated von Bertalanffy growth parameters, as well as the Akaike's information criterion corrected for small samples for the three methods are represented in Table 3.3. The von Bertalanffy growth parameters were quite different between methods, with whole otolith approach and combined methodology (CM) presenting the lowest (41.888 cm) and highest (45.704 cm) values of L_∞, respectively. The highest k value (0.293) was obtained for the whole otolith method and the lowest value (0.199) for CM, while the highest t_0 (-1.455 yr) was obtained using BC method and the lowest t_0 (-0.532 yr) was obtained for the whole otolith method. The von Bertalanffy growth curves for *T. lyra* are presented in Figure 3.7.

Table 3.3. von Bertalanffy growth parameters estimated for *Trigla lyra*, using three different methods: whole otolith reading, back-calculation (BC), and a combination of the previous two methodologies (CM). Standard error of parameters is given in parenthesis.

Method	Von Bertalanffy growth parameters			c-AIC
	$L\infty$ (cm)	k	t_0 (yr)	
Whole otolith	41.888 (2.980)	0.293 (0.091)	- 0.532 (0.564)	58.0
BC	42.579 (1.216)	0.204 (0.021)	- 1.455 (0.233)	27.9
CM	45.704 (1.952)	0.199 (0.029)	- 1.302 (0.309)	36.4

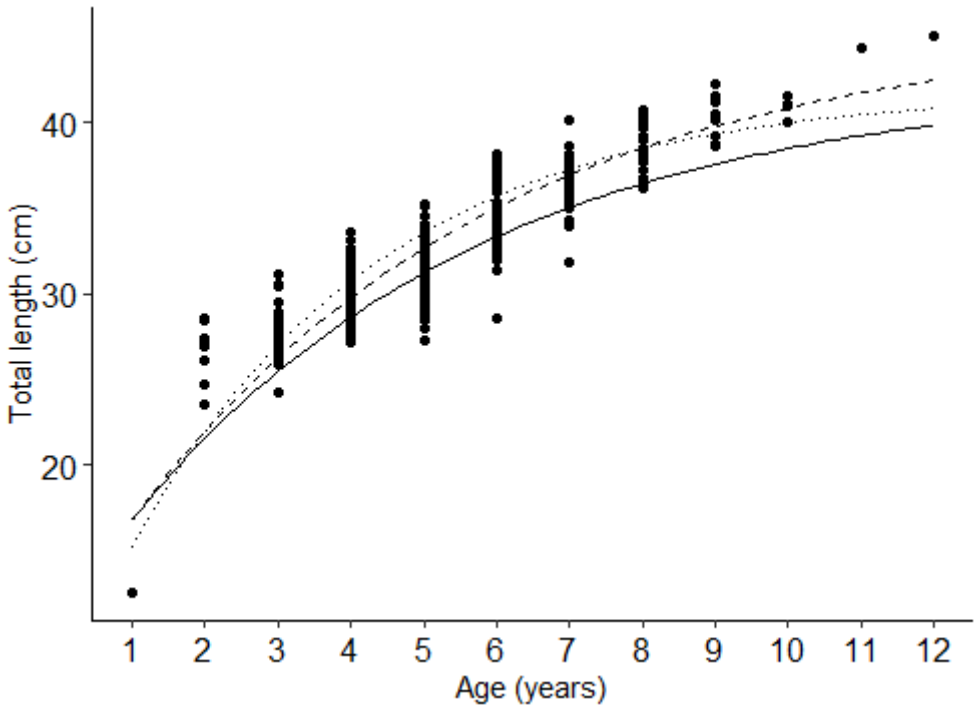

Fig. 3.7. The von Bertalanffy growth curves for *Trigla lyra* using three different methods: whole otolith reading (dotted line), back-calculation (dashed line), and combined methodology (continuous line).

3.3. Reproduction

The gonads of *T. lyra* presented macroscopic differences between sexes, although there were some common features between ovaries and testes. Both gonads appeared in the abdominal cavity in pairs, were located ventrally relative to the swim bladder and posteriorly in the abdominal cavity. Also, they were fused at their posterior ends,

anteriorly to the urogenital opening (Fig. 3.8). The macroscopic aspect of the gonads varied throughout the reproductive cycle. Ovaries in developing phase were small, had a transparent to pinkish coloration and did not present oocytes visible by the naked eye. Spawning capable females had larger and more vascularized ovaries, with visible oocytes and an orange to yellowish coloration. Actively spawning phase was characterized by the presence of large ovaries filling almost all the abdominal cavity of the fish, the presence of transparent and larger oocytes comparing with the previous phase, with the release of some oocytes and jelly, and prominent blood vessels. Lastly, after spawning (namely in regressing and regenerating phases) the ovaries were flaccid and considerably smaller, with no visible oocytes and a dark pinkish to transparent coloration. Regarding males, testes in developing phase were very small, thin and flaccid, with whitish coloration and sometimes very hard to distinguish. In its turn, spawning capable males presented larger and thicker testes occupying a larger part of the abdominal cavity, opaquer and whiter, and occasionally releasing sperm. Finally, regressing testes had characteristics like developing testes, although more transparent and thinner.

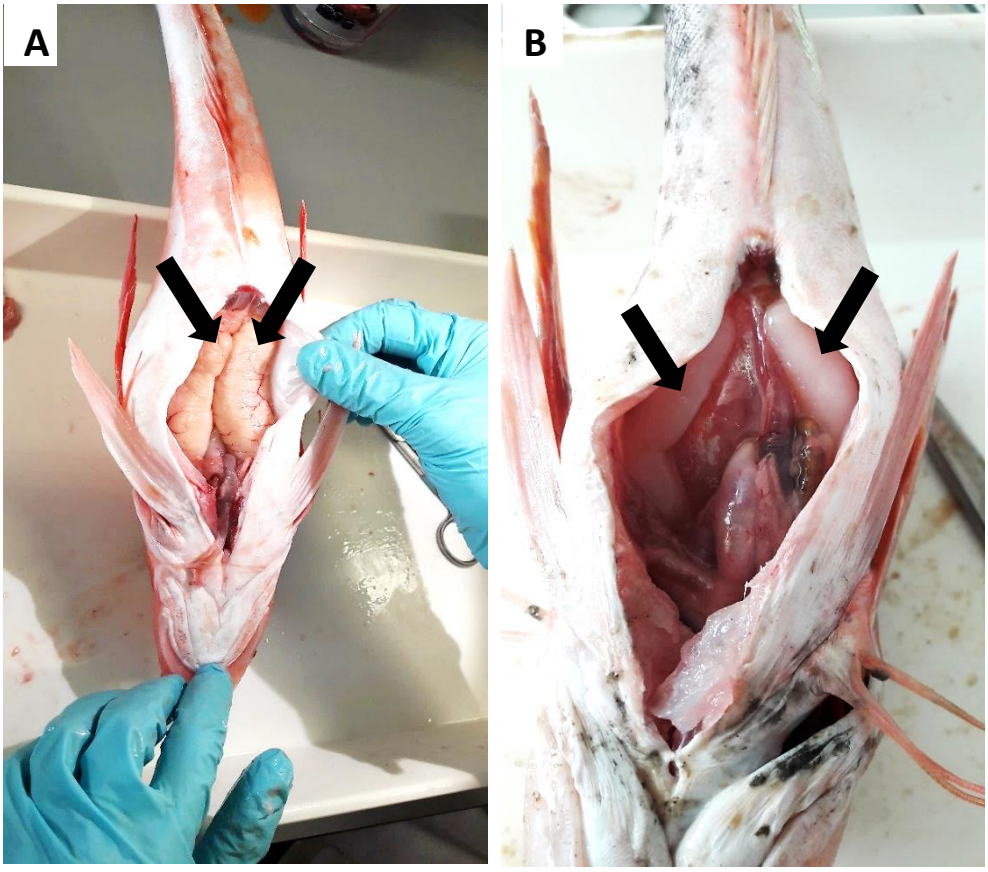

Fig. 3.8. Actively spawning female (A) and spawning capable male (B) of *Trigla lyra*. The gonads, ovaries (A) and testes (B), are pointed out with black arrows.

Macroscopic characteristics of the gonads allowed to establish a macroscopic maturity scale for *T. lyra* (Table 4.1.), based on the terminology proposed by Brown-Peterson et al. (2011).

Table 3.4. Macroscopic maturity scale for *Trigla lyra*, based on the terminology proposed by Brown-Peterson et al. (2011).

Maturity phase	Females	Males
Developing (De)	Small ovaries, with a transparent to pinkish coloration. Oocytes are not visible by the naked eye.	Small, thin and flaccid testes, with whitish coloration and sometimes very hard to distinguish.
Spawning capable (SC)	Larger and more vascularized ovaries, with an orange to yellowish coloration. Oocytes are visible by the naked eye.	Larger and thicker testes occupying a larger part of the abdominal cavity, opaquer and whiter, and occasionally releasing sperm.
Actively spawning (AS; subphase)	Large ovaries filling almost all the abdominal cavity of the fish. Presence of transparent and larger oocytes comparing with the previous phase, visible by the naked eye. Release of some oocytes and jelly. Prominent blood vessels.	
Regressing (RG)	Ovaries considerably smaller than in AS phase and flaccid, with a dark pinkish to transparent coloration. Oocytes are not visible by the naked eye. Blood vessels may be visible.	Small and flaccid testes, and thinner than in De phase. Transparent coloration.
Regenerating (RN)	Ovaries smaller than in RG phase and flaccid. Oocytes are not visible by the naked eye. Blood vessels hardly visible.	

3.3.1. Sex ratio

Regarding sex ratio, there were significant differences from 1/1 ratio (χ^2 = 112.17, df = 19, $p < 0.05$), with females being predominant in relation to males (sex ratio of 3.46/1). Sex ratio was significantly biased towards females in all months of sampling except in May 2018, October 2018, April 2019 and May 2019 (Table 3.4). April 2019 was the only month where the number of females was the same as the number of males.

Table 3.5. Summary of the Chi-squared test made to check for significant differences from 1/1 ratio in sex ratio of *Trigla lyra*, for each month of sampling.

Month	Chi-squared test	Sex ratio (females/males)
May 2018	χ^2 = 3.81, df = 1, p = 0.1449	9/1
September 2018	χ^2 = 5.32, df = 1, p = 0.0420	2.69/1
October 2018	χ^2 = 3.20, df = 1, p = 0.1079	1.91/1
November 2018	χ^2 = 18.67, df = 1, p = 0.0005	No males
December 2018	χ^2 = 46.55, df = 1, p = 0.0005	74/1
January 2019	χ^2 = 5.37, df = 1, p = 0.0315	1.97/1
February 2019	χ^2 = 18.38, df = 1, p = 0.0005	4.64/1
March 2019	χ^2 = 7.41, df = 1, p = 0.0105	4.14/1
April 2019	χ^2 = 0, df = 1, p = 1	1/1
May 2019	χ^2 = 3.45, df = 1, p = 0.1119	2.75/1

3.3.2. Structure of the gonads

All stages of oocyte development were identified in females: primary growth (PG), cortical alveolar (CA), primary and secondary vitellogenic (<Vtg3), tertiary vitellogenic (Vtg3), oocyte maturation (OM) (Fig. 3.9) and hydrated (H) (Fig. 3.10B). There was an increase in oocyte diameter from the PG stage to H stage, ranging from 37 µm to 1690.1 µm (Fig. 3.12, Table 3.5). Furthermore, atresia (Fig. 3.9D), which constituted the process of degeneration and resorption of an oocyte, and POFs (Fig. 3.10A), constituting the remnant follicle in the ovary after ovulation, were also observed in several ovaries.

Regarding males, all four stages of development of spermatogenesis were identified: spermatogonia (Sg), spermatocytes (Sc), spermatids (St), and spermatozoids (Sz) (Fig.

3.11). The development of cells occurred inside spermatocysts (Sp; Fig. 3.11A, C), which in turn were organized into lobules in the testis (L; Fig. 3.10A). As opposed to females, there was a decrease in the diameter of male cells from Sg stage to Sz stage (Fig. 3.13, Table 3.6). The diameter of male sexual cells varied between 1.9 and 10.2 µm.

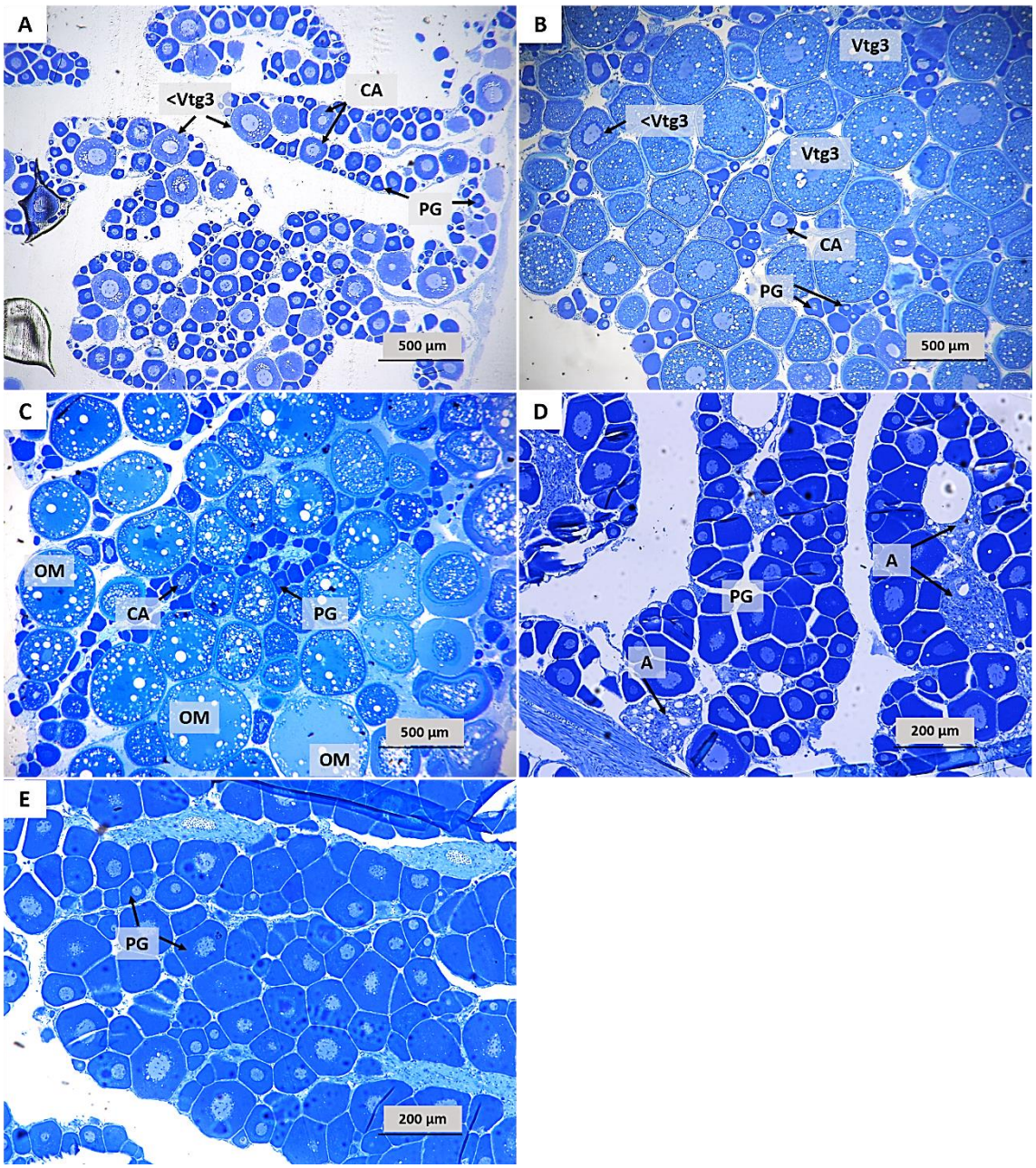

Fig. 3.9. Transverse sections of ovaries of *Trigla lyra*. (A) Developing female; (B) spawning capable female; (C) actively spawning female; (D) regressing female; (E) regenerating female. PG, primary growth oocyte; CA, cortical alveolar oocyte; <Vtg3, primary and secondary vitellogenic oocytes; Vtg3, tertiary vitellogenic oocyte; OM, oocyte maturation; A, atresia.

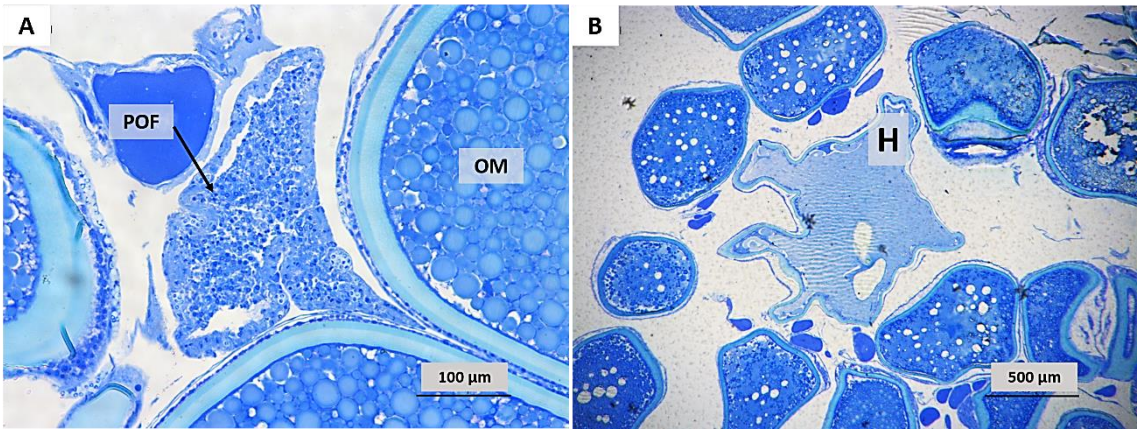

Fig. 3.10. (A) Post-ovulatory follicle in an actively spawning female; (B) hydrated oocyte in an actively spawning female. OM, oocyte maturation; H, hydrated oocyte; POF, post-ovulatory follicle.

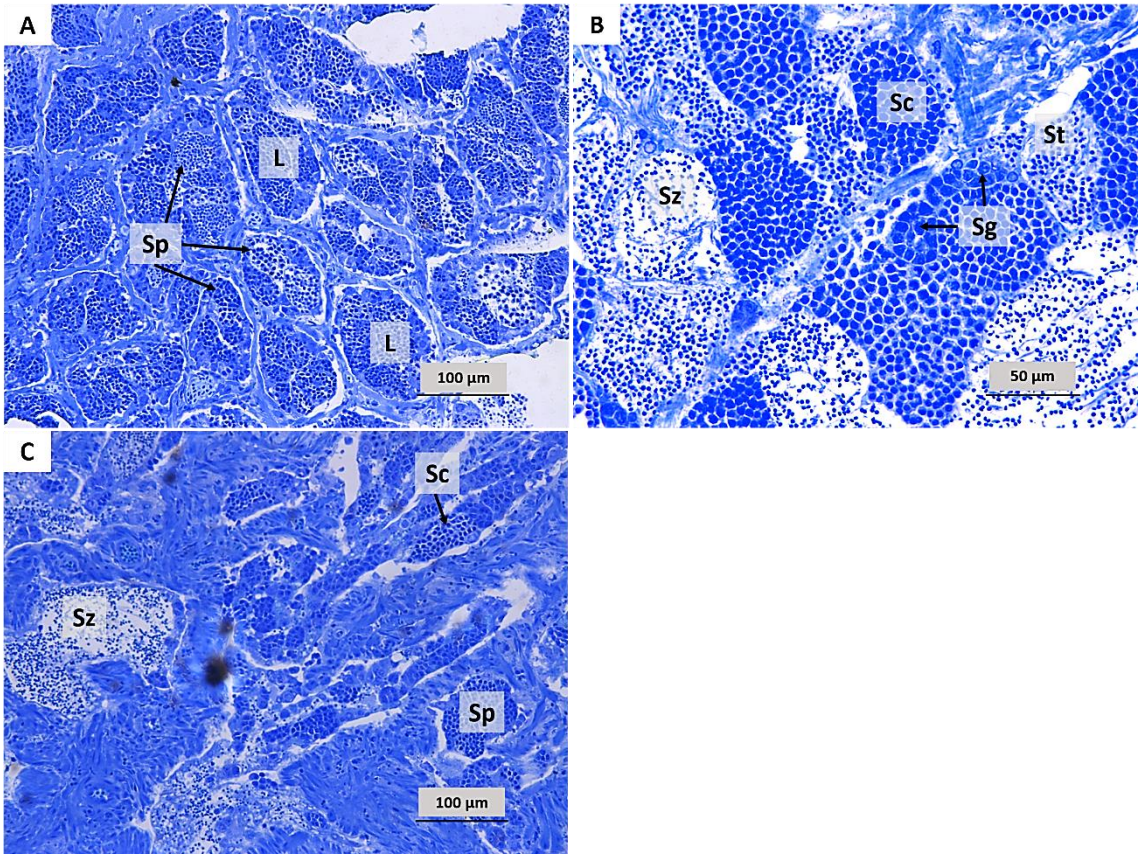

Fig. 3.11. Transverse sections of testes of *Trigla lyra*. (A) Developing male; (B) spawning capable male; (C) regressing male. Sg, spermatogonia; Sc, spermatocytes; St, spermatids; Sz, spermatozoa; Sp, spermatocysts; L, lobule.

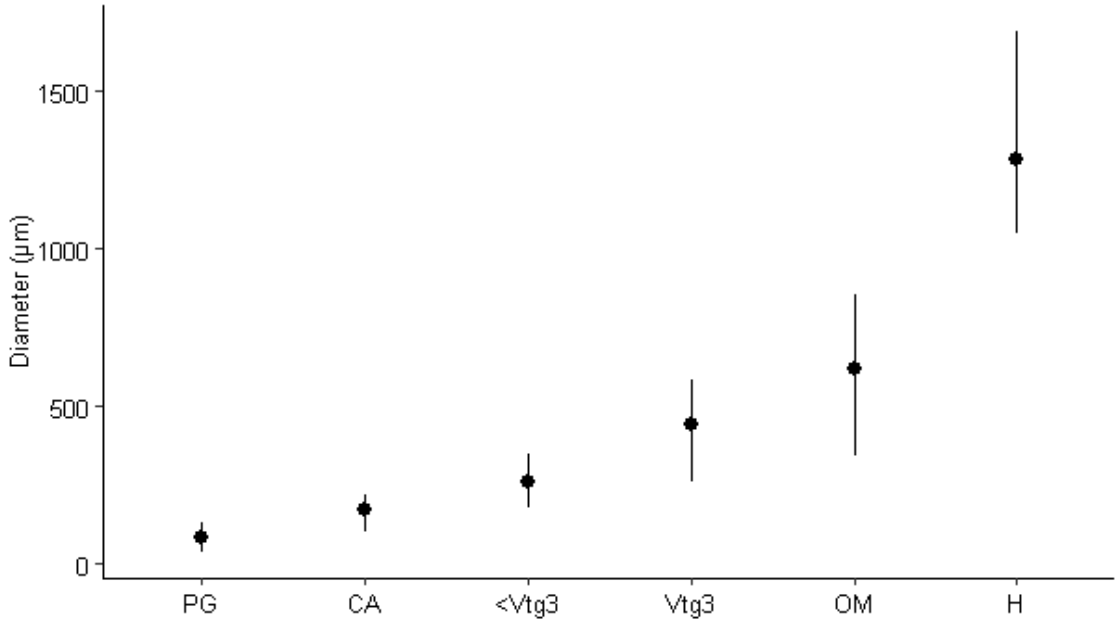

Fig. 3.12. Variation of the mean diameter (µm) of oocyte stages of oogenesis: primary growth (PG), cortical alveolar (CA), primary and secondary vitellogenic (<Vtg3), tertiary vitellogenic (Vtg3), oocyte maturation (OM) and hydrated (H).

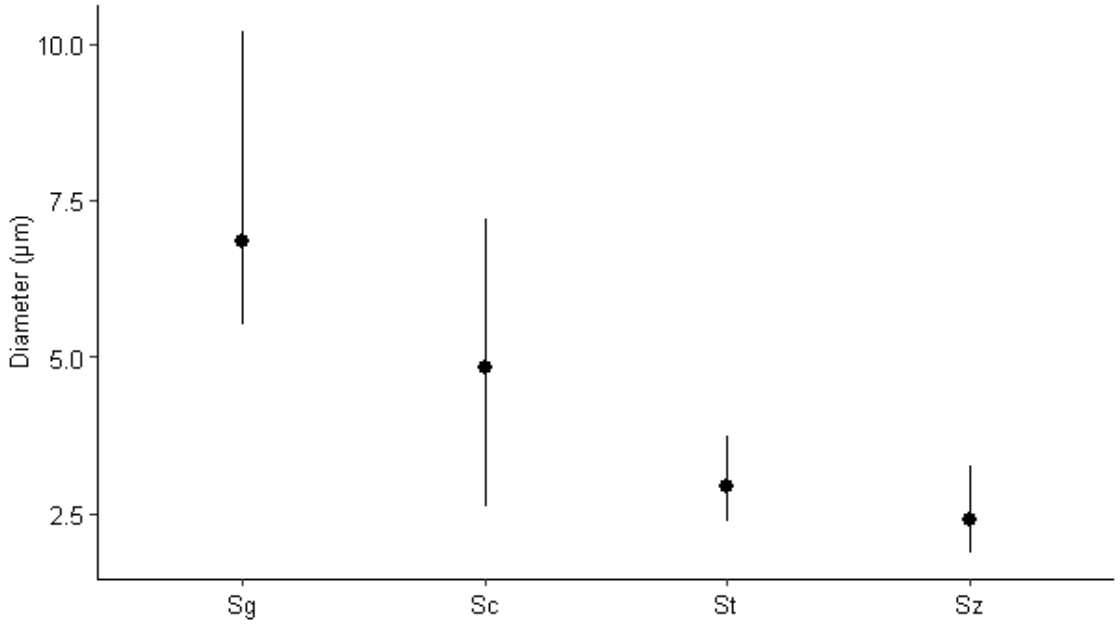

Fig. 3.13. Variation of the mean diameter (µm) of male cells: spermatogonia (Sg), spermatocytes (Sc), spermatids (St), and spermatozoids (Sz).

Table 3.6. Summary of oocyte stages of oogenesis for *T. lyra*. Values of minimum and maximum diameter for each stage are given, with mean and standard deviation between brackets. N – number of oocytes measured.

Oocyte stage	Description	Diameter (µm)	N
Primary growth (PG)	Polyhedral form, highly stained basophilic cytoplasm.	37.0-130.3 (81.7 ± 24.1)	100
Cortical alveolar (CA)	Lighter cytoplasm than in PG stage and more granular. Cortical alveoli appear in the periphery of the cytoplasm, and oil droplets may be present in some oocytes.	100.0-219.1 (171.0 ± 22.6)	109
Primary and secondary vitellogenic (<Vtg3)	Yolk granules appear in the cytoplasm and oil droplets increase in size and number.	179.1-346.5 (257.0 ± 43.3)	105
Tertiary vitellogenic (Vtg3)	Large yolk granules and lipid droplets occupy all the cytoplasm.	262.2-583.5 (441.1 ± 78.8)	106
Oocyte maturation (OM)	Nucleus migrates, yolk granules fuse to form a continuous mass, and in some oocytes the oil droplets also fuse.	340.4-852.9 (620.1 ± 152.1)	69
Hydrated (H)	Irregular form, cytoplasm filled with fluid. These oocytes are ready to be released.	1049.1-1690.1 (1282.3 ± 150.2)	153

Table 3.7. Summary of male cells stages for *T. lyra*. Values of minimum and maximum diameter for each stage are given, with mean and standard deviation between brackets. N – number of male cells measured.

Male cells stage	Description	Diameter (µm)	N
Spermatogonia (Sg)	Appear alone or in small groups. Polyhedral form, visible cytoplasm and large nucleus.	5.5-10.2 (6.9 ± 1.0)	56
Spermatocytes (Sc)	Appear enclosed in spermatocysts. Spherical form, smaller than Sg.	2.6-7.2 (4.8 ± 1.3)	124
Spermatids (St)	Appear also enclosed in spermatocysts. Smaller than Sc, with nucleus not visible.	2.4-3.7 (2.9 ± 0.2)	80
Spermatozoids (Sz)	Appear enclosed in spermatocysts or free in the lumen of lobules. Very similar to St but present cilia.	1.9-3.2 (2.4 ± 0.3)	101

3.3.3. Sexual cycle and spawning season characterization

All maturity phases of the reproductive cycle were identified in females: developing (De), spawning capable (SC), actively spawning (AS), regressing (RG), and regenerating (RN). Developing individuals occurred mainly in September 2018 and October 2018, while actively spawning individuals appeared between November 2018 and March 2019, being predominant in January 2019. Individuals in regressing phase occurred in May 2018, and between February 2019 and May 2019, showing the highest percentage in March 2019. Regenerating individuals were observed in May 2018, April 2019 and May 2019 (Fig. 3.14A).

In males, not all maturity phases were present. Developing individuals appeared from May 2018 to December 2018 and were predominant in September 2018. The months of May 2018 and December 2018 were not representative in terms of males because only one individual was sampled in each month. Specimens in spawning capable phase appeared between September 2018 and October 2018, as well as between January 2019 and April 2019. All individuals sampled in May 2019 were in regressing phase. Finally, the regenerating phase was not observed (Fig. 3.14B).

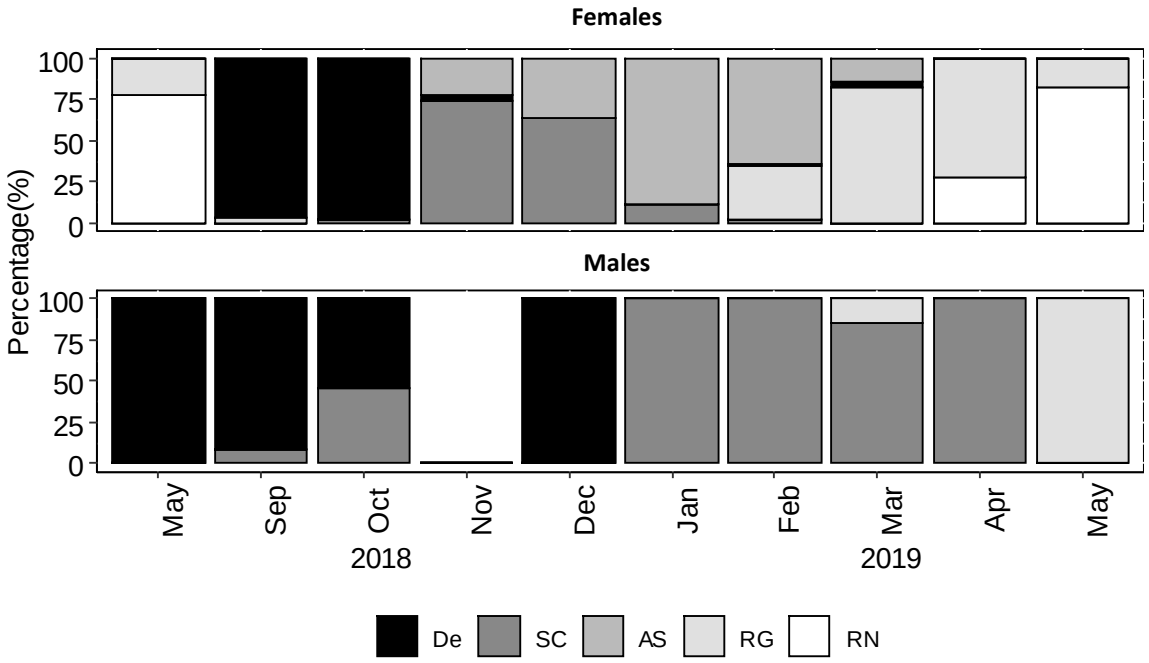

Fig. 3.14. Percentage of different maturation phases through the sampling period for females (A) and males (B) of *Trigla lyra*. De, developing; SC, spawning capable; AS, actively spawning; RG, regressing; RN, regenerating.

The evolution of the GSI, HSI and K for both sexes throughout the months of sampling is represented in Figure 3.15. Female GSI increased from September 2018 to January 2019, reaching a maximum value of 14.46 %, and then decreased until May 2019 (0.63 %). Male GSI presented a similar pattern, although its highest value was in February 2019 (2.91 %). Female HSI increased from May 2018 (lowest value, 1.32 %) to January 2019 (3.63 %), and then decreased until May 2019. Male HSI decreased from September 2018 (highest value of 3.28 %) until October 2018, and then decreased from December 2018 to April 2019, reaching the lowest value of 1.31 %. In terms of the variation of K, there was an increasing trend in female K from May 2018 until January 2019 (highest value of 0.83 %). Male K decreased from September 2018 to February 2019, increasing then until April 2019. The lowest (0.63 %) and highest (0.79 %) values of male K were verified in May and September 2018, respectively. There were no values for males in November 2018 because there was no occurrence of males in that month. The Kruskal-Wallis test indicated significant differences in the indices' values among months, for both sexes ($p < 0.05$). Female GSI and male GSI presented differences, specially between January and February and the other months (Tukey-test).

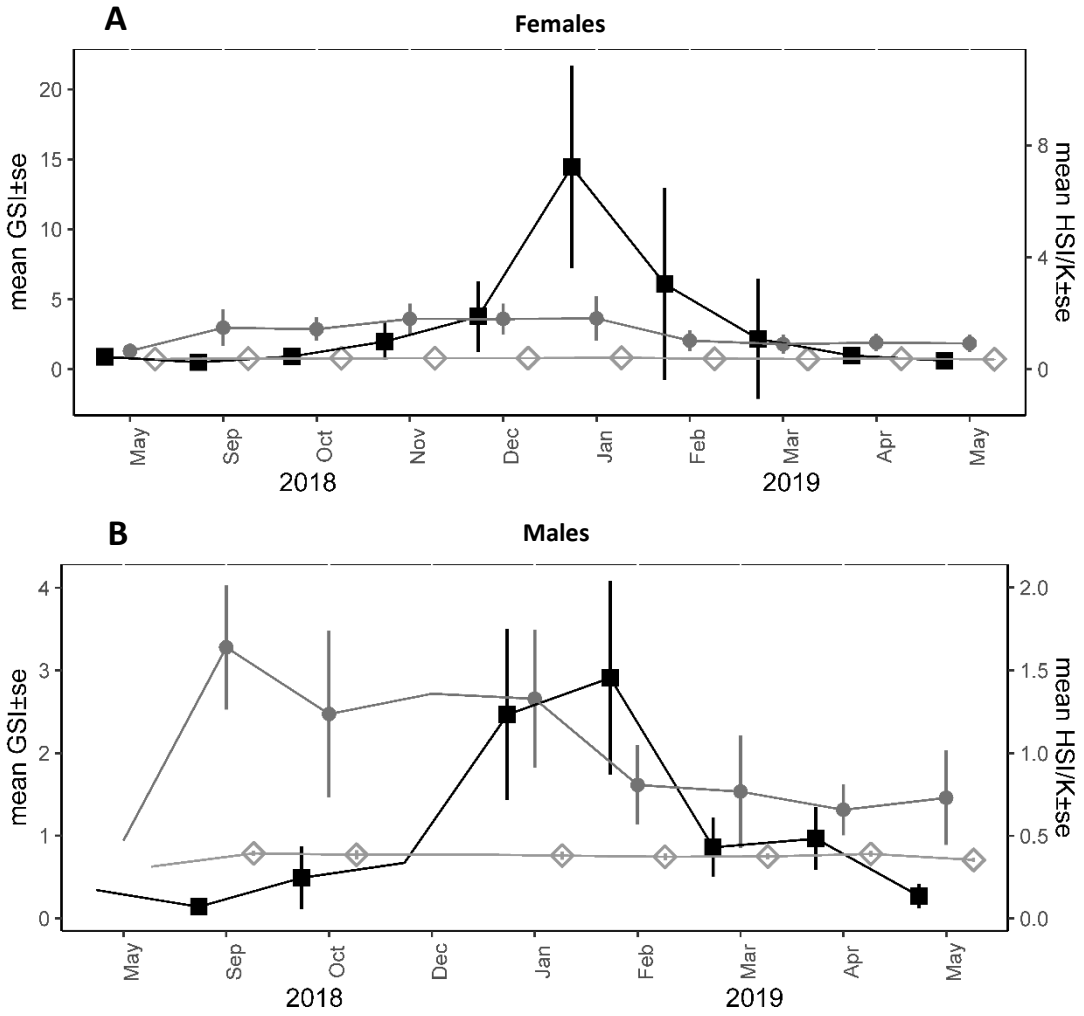

Fig. 3.15. Monthly evolution of the mean and standard error of gonadosomatic index (GSI) (black squares), hepatosomatic index (HSI) (grey circles) and Fulton's condition factor (K) (open diamonds) for females (A) and males (B) of *Trigla lyra*.

Regarding the evolution of indices' values among maturity phases in the reproductive cycle (Fig. 3.16), female GSI was higher in individuals in AS phase (10.63 %) and lower in RN individuals (0.69 %). Male GSI was higher in individuals in SC phase (1.90 %) and lower in developing individuals (0.32 %). The Kruskal-Wallis test indicated significant differences in female GSI among maturity phases of the reproductive cycle ($p < 0.05$), particularly between SC and AS and the other phases (De, RG, RN) (Tukey-test). For males, significant differences in GSI between maturity phases were found ($p < 0.05$), namely between SC and the other phases (De and RG) (Tukey-test). With respect to HSI, females presented the highest value in SC phase (3.39 %), followed by a decrease until RG phase (lowest value, 1.71 %). In turn, male HSI varied between 2.67 % in De phase (highest value) and 1.39 % (lowest value) in RG phase. Female K varied from 0.73 %

(lowest value) in RN phase and 0.81 % (highest value) in AS phase, whilst male K varied between 0.71 % (lowest value) in RG phase and 0.77 % (highest value) in De phase. Female HSI and K were significantly different among reproductive phases ($p < 0.05$). Significant differences were also found for male HSI and K ($p < 0.05$) among reproductive phases, namely between RG phase and the other two phases.

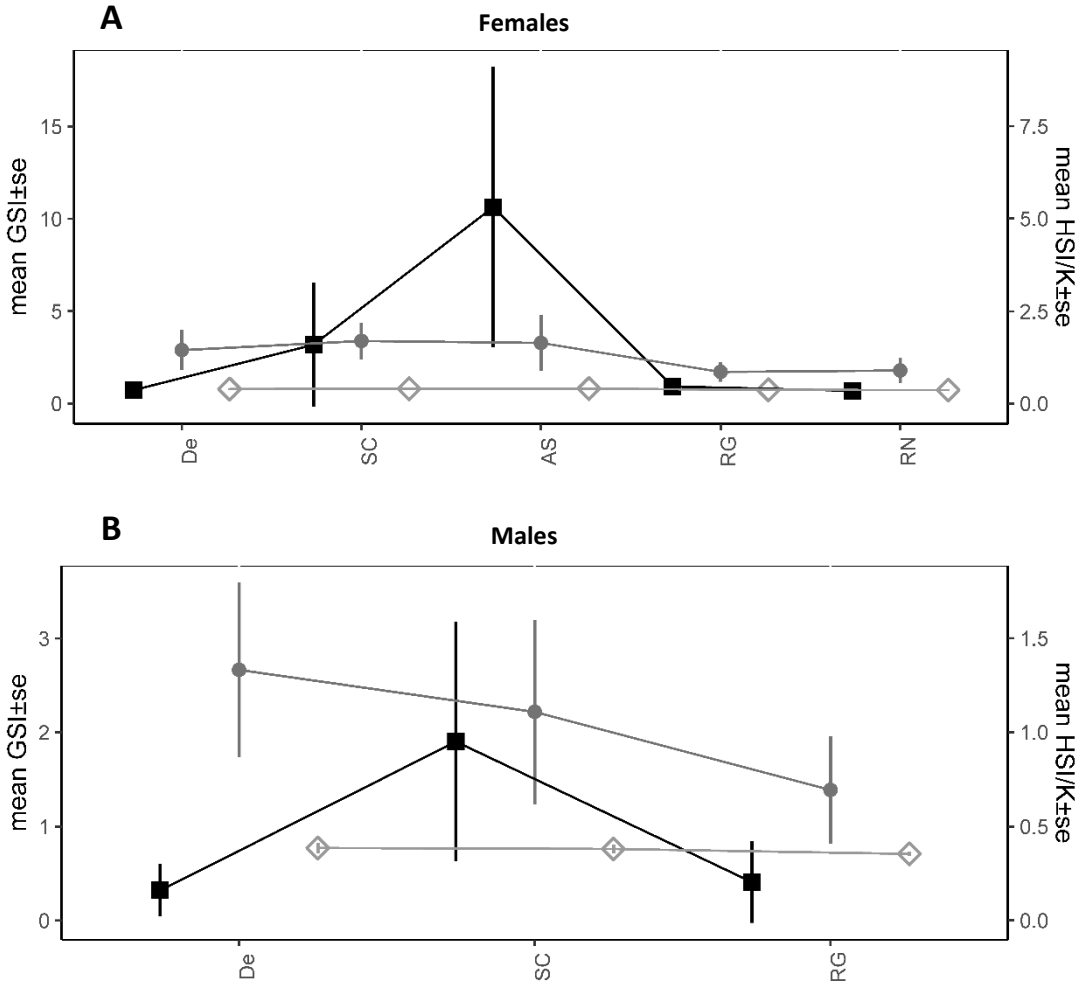

Fig. 3.16. Evolution among maturity reproductive phases of the mean and standard error of gonadosomatic index (GSI) (black squares), hepatosomatic index (HSI) (grey circles) and Fulton's condition factor (K) (open diamonds) for females (A) and males (B) of *Trigla lyra*. De, developing; SC, spawning capable; AS, actively spawning; RG, regressing; RN, regenerating.

Regarding the results obtained, November 2018 was the first month when the percentage of females in SC phase or pre spawning condition was higher than 50 %, which points out the beginning of the spawning season. In March 2019, more than 50 % of females

were in RG phase or post spawning condition (Fig. 3.14A). However, only 4 out of 29 females were in AS phase, while 24 females were in RG phase. Furthermore, in the second date of February more than 50 % of females were already in RG phase. The evolution of the gonadosomatic index indicated higher values from November to March in females (Fig. 3.15A) and higher values from December to April in males (Fig. 3.15B). Given this, the duration of the spawning season was defined as the period between November and February. The peak of spawning corresponded to January 2019 as it presented the highest proportion of AS females (Fig. 3.14A) and a higher GSI for females (Fig. 3.15A).

3.3.4. Fecundity

Regarding the homogeneity among (between medium, anterior and posterior regions) and between ovaries, no significant differences in the distribution of oocytes were obtained ($p > 0.05$).

Regarding the first line of evidence, the results show the formation of a gap between the group of least advanced oocytes and the group of most advanced oocytes, throughout the months of the spawning season. A gap between the unyolked oocytes (< 194 µm) and the yolked oocytes/mature oocytes (> 214 µm) started to appear in January 2019, indicating the existence of a hiatus (Fig. 3.17). Oocyte size-frequency distribution in the different phases of the reproductive cycle (Fig. 3.18) shows an increase in the percentage of yolked oocytes and mature oocytes (> 214 µm) from the developing phase to the actively spawning phase, followed by a decrease in the regressing phase. Regressing females only present unyolked oocytes.

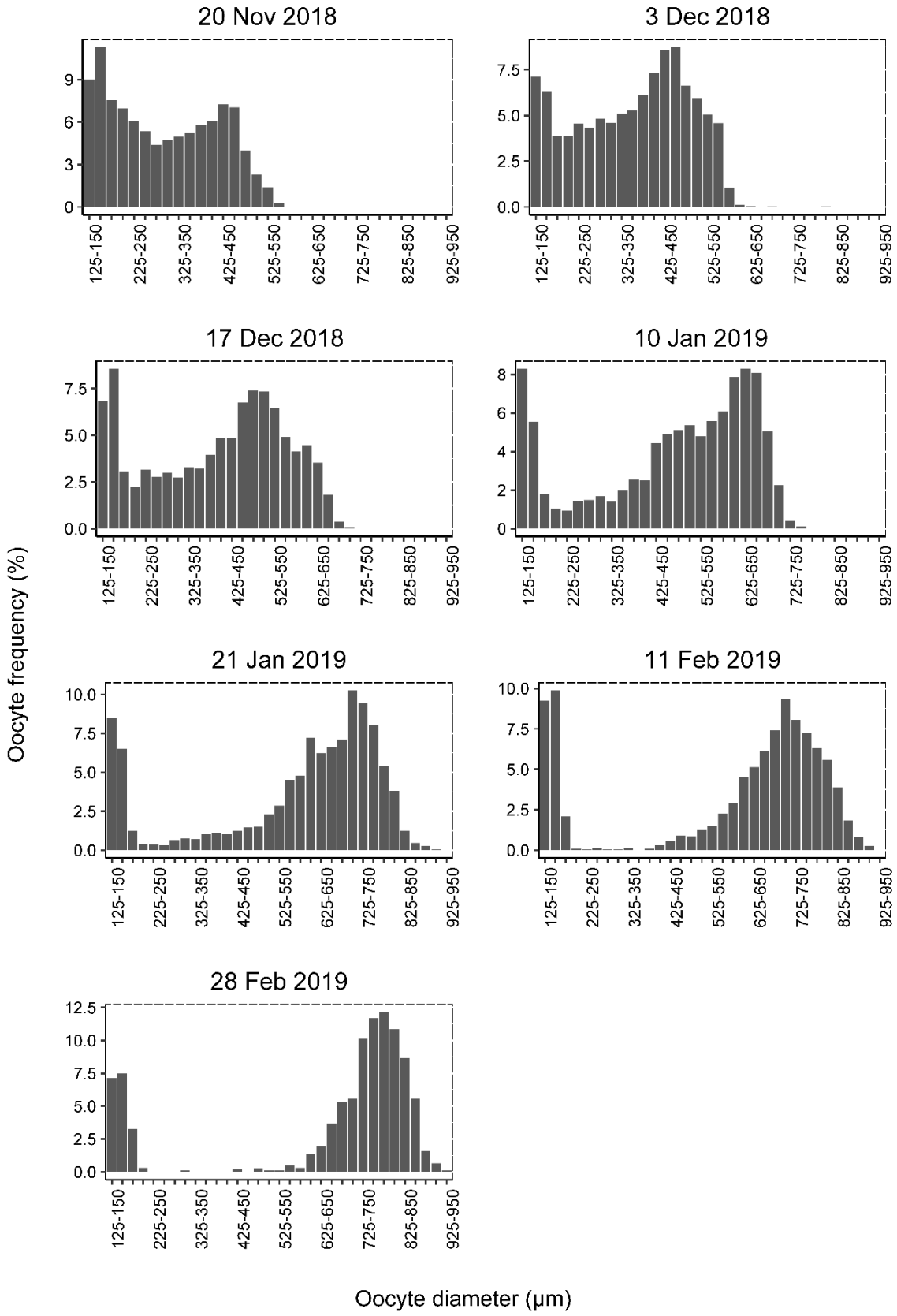

Fig. 3.17. Oocyte size-frequency distribution during the spawning period for *Trigla lyra*. Oocyte diameter classes of 25 µm were used.

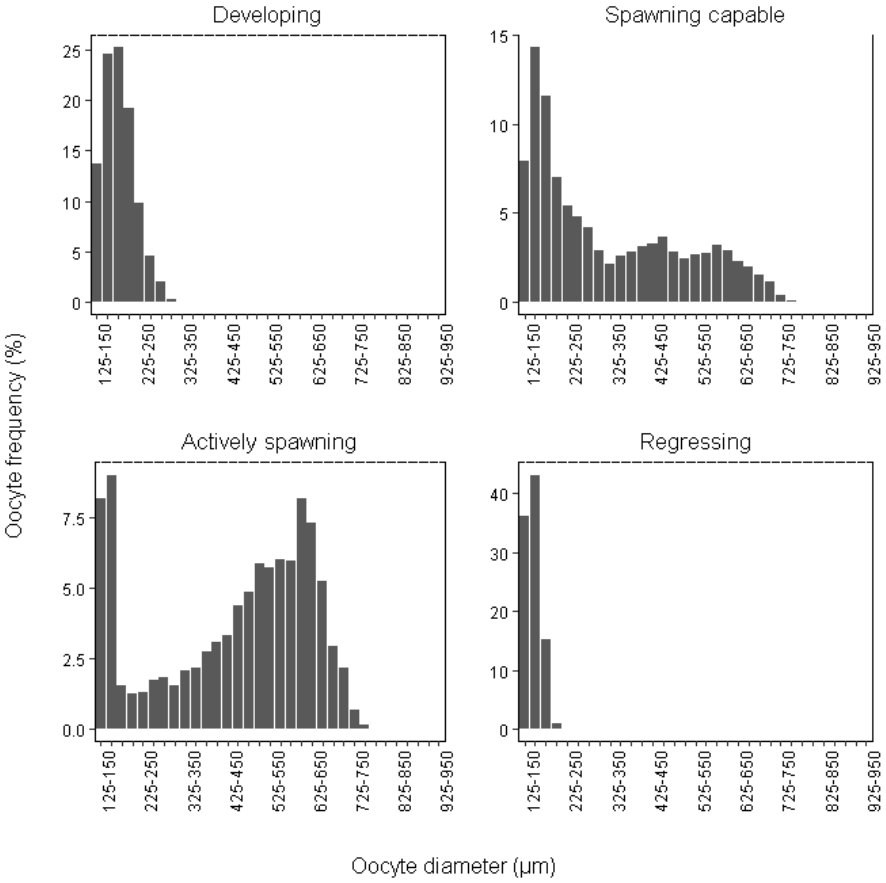

Fig. 3.18. Oocyte size-frequency distribution for developing, spawning capable, actively spawning and regressing females of *Trigla lyra*. Oocyte diameter classes of 25 µm were used.

Regarding the second criteria, a decreasing trend in the number of advanced vitellogenic oocytes (Vtg3, 360-520 µm) along the spawning season was observed, except between November and the first date of December (3 Dec) (Fig. 3.19). Significant differences in the number of Vtg3 between months of the spawning season were obtained (KW = 24.23, $p < 0.05$)

With respect to the third criteria, an increasing tendency in the mean diameter of advanced yolked oocytes (Vtg3, 360-520 µm) over the spawning season was verified, except between 10 January and 21 January (Fig. 3.20). It varied between 431.4 µm in November and 465.9 µm in 28 February. However, the Kruskal-Wallis test didn't detect significant differences in the mean diameter by month (KW=11.119, $p < 0.05$).

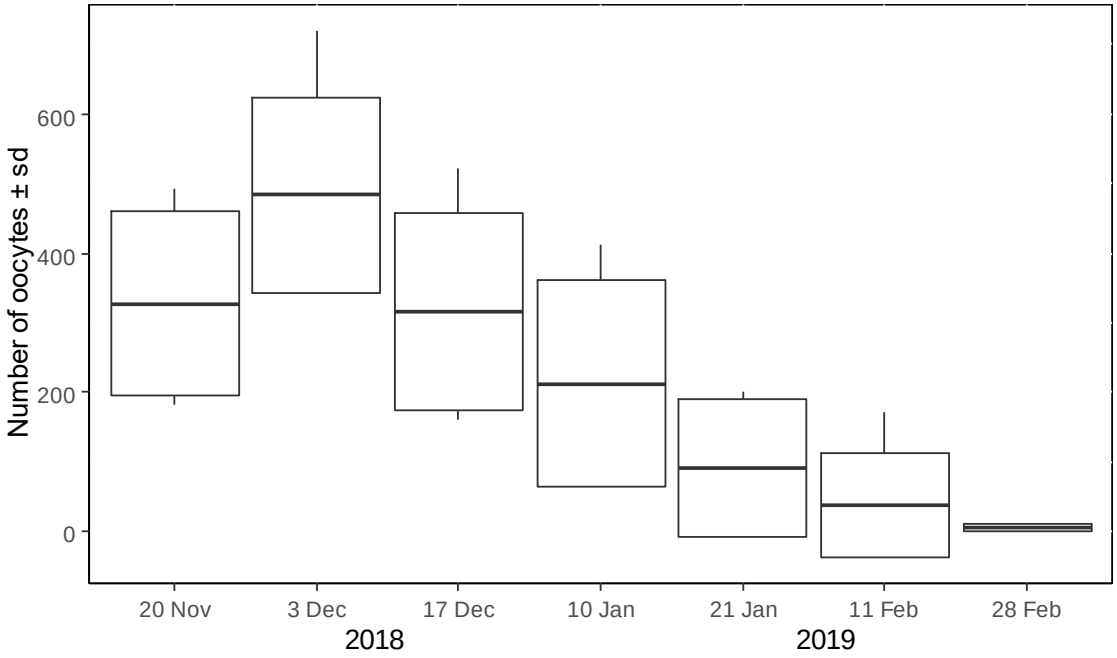

Fig. 3.19. Monthly variation of the number of advanced vitellogenic oocytes (Vtg3) over the spawning season.

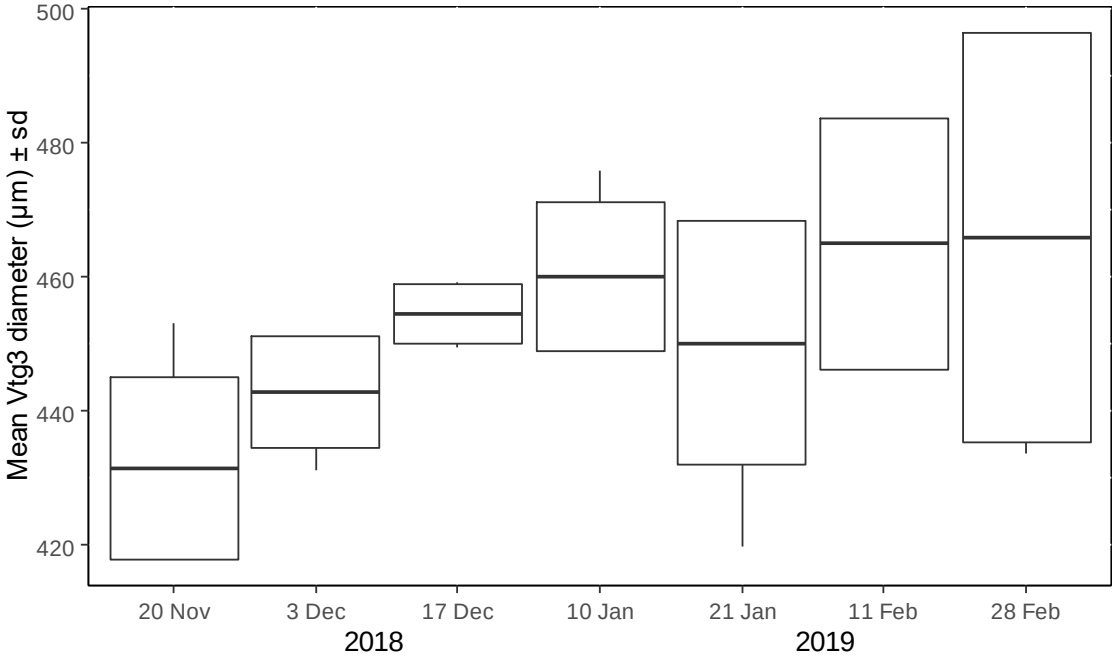

Fig. 3.20. Monthly variation of the mean diameter of advanced vitellogenic oocytes (Vtg3) over the spawning season.

Finally, atresia prevalence throughout the spawning season varied between 27.0 % in January 2019 and 55.3 % in February 2019, with a mean of 43.7 % (Fig. 3.21). No massive atresia occurred at the end of the spawning season.

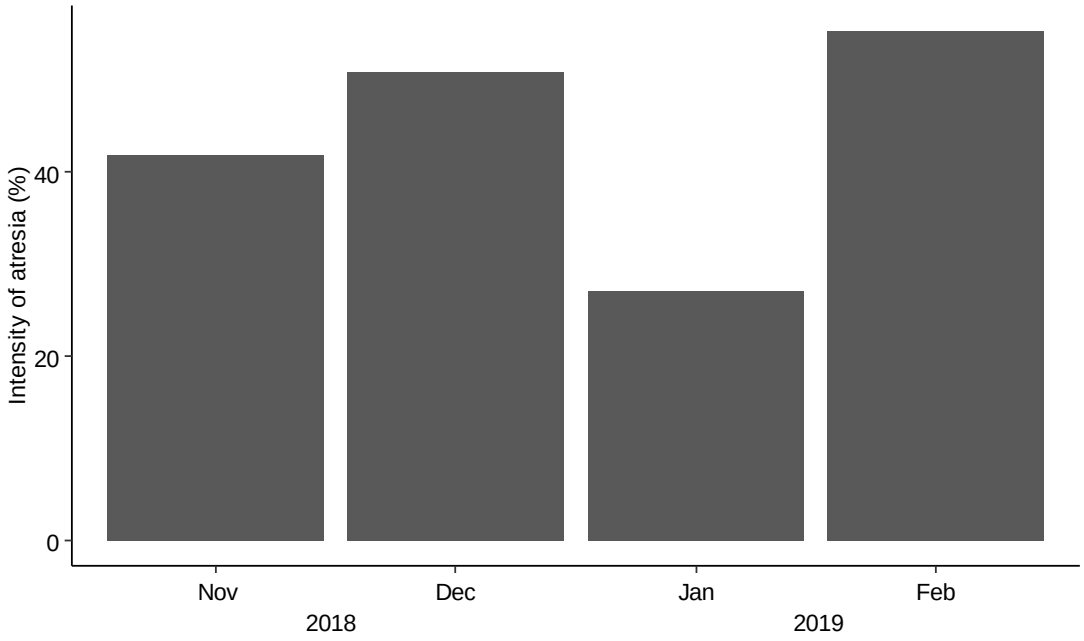

Fig. 3.21. Monthly variation of the intensity of atresia in the ovaries through the spawning period for *Trigla lyra*.

3.4. Chemical composition of the muscle

The variation in the chemical composition of the muscle of *T. lyra* is shown in Figure 3.22, and the results suggest that water is the main component, followed by proteins, ash and lipids (equivalent to total fat). The lowest value of protein content was 16.55 % in January and the highest was 17.65 % in March. Total fat decreased from January (1.73 %) to March (0.74 %), and then increased until May (1.11 %). Regarding moisture, it decreased from January (74.49 %) to March (68.81 %), then increasing until May (73.52 %). Finally, ash content increased from January (6.17 %) until May (10.09 %).

Kruskal-Wallis test indicated that there were significant differences in protein content and total fat among months ($p < 0.05$). Total fat was significantly different between January and March, while protein content differed significantly between January and May (Tukey-test). On the other hand, the month did not influence ash content neither moisture.

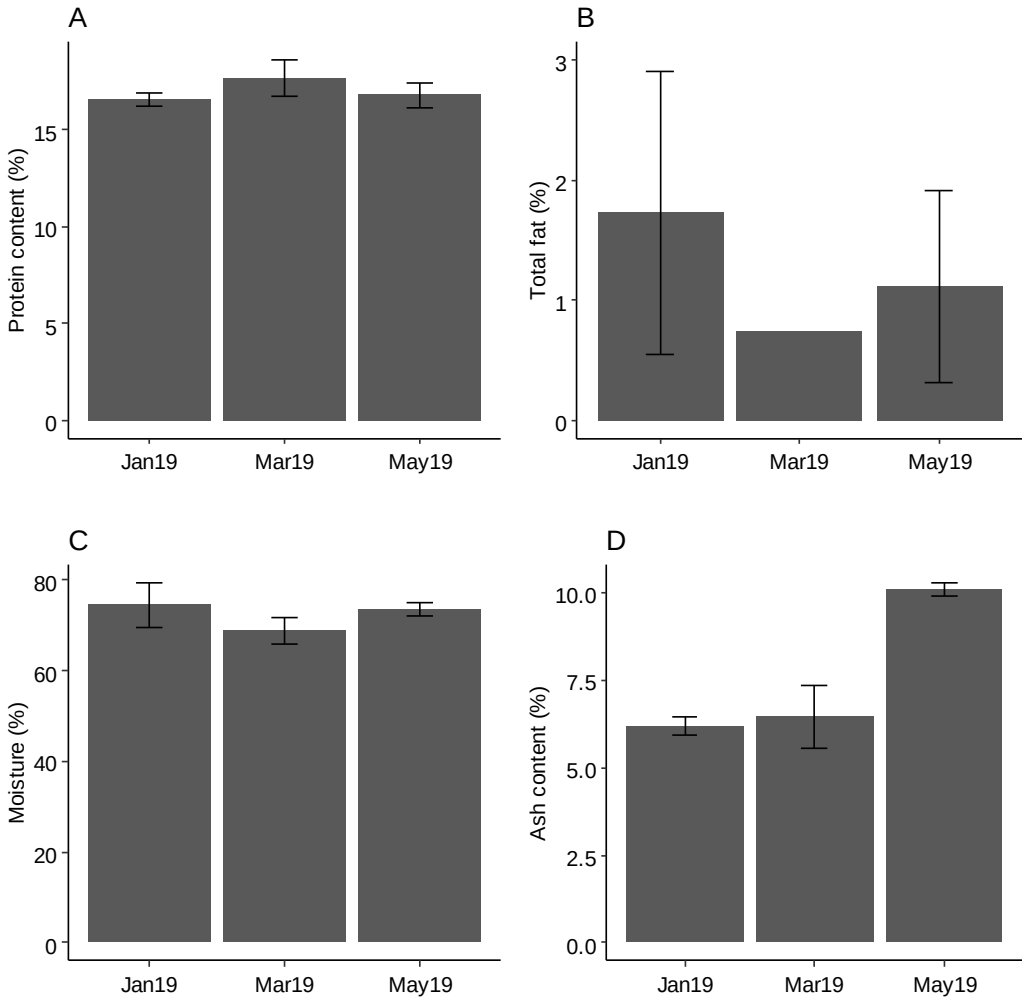

Fig. 3.22. Monthly variation of the chemical composition in the muscle of *Trigla lyra* in 2019. Protein content (A); total fat (B); relative moisture (C); ash content (D). The values of protein content and total fat are expressed in 100g of fresh sample.

Fatty acids composition of *T. Lyra* is shown in Table 3.7, where a total of 21 fatty acids were identified. Saturated fatty acids (SFAs), monounsaturated fatty acids (MUFAs) and polyunsaturated fatty acids (PUFAs) were part of the composition of *T. lyra*. It was notorious that May 2019 presented the highest quantity of fatty acids. SFAs were the main constituents in January (mean value of 6.67 mg/g), while MUFAs were the main components in March (10.33 mg/g) and PUFAs were the principal components in May (15.56 mg/g). Within the group of SFAs, palmitic acid (C16) was the most abundant, and within the group of MUFAs, oleic acid (C18:1n9c) was the predominant fatty acid. Amongst PUFAs, ω-3 fatty acids presented the highest concentrations, namely docosahexaenoic acid (DHA) (highest concentration) and eicosapentaenoic acid (EPA).

The composition in stearic acid (C18), lignoceric acid (C24), EPA, DHA and AA differed significantly between months ($p < 0.05$). Pentadecenoic acid (C15:1), oleic acid (C18:1n9c) and palmitoleic acid (C16:1) differed significantly between May and the other two months.

Table 3.8. Mean fatty acids composition of the muscle of *Trigla lyra* analysed in January, March and May 2019 (mg/g). SFAs, saturated fatty acids; MUFAs, monounsaturated fatty acids; PUFAs, polyunsaturated fatty acids; ALA, α-linoleic acid; EPA, eicosapentaenoic acid; DPA, docosapentaenoic acid; DHA, docosahexaenoic acid; LA, linoleic acid; AA, arachidonic acid. Values are expressed as mean ± SD (n = 3). Means in the same row with unlike letters differ significantly ($p < 0.05$).

Fatty acids	*January 2019*	*March 2019*	*May 2019*
C8	0.28 ± 0.01	0.58 ± 0.06	0.39 ± 0.01
C10	0.30 ± 0.02	0.47 ± 0.00	0.35 ± 0.03
C12	0.15 ± 0.01	0.34 ± 0.05	0.21 ± 0.03
C14	0.66 ± 0.04	0.97 ± 0.10	1.44 ± 0.05
C15	0.21 ± 0.02	0.27 ± 0.03	0.44 ± 0.01
C16	3.47 ± 0.14	4.50 ± 0.43	8.23 ± 0.16
C17	0.15 ± 0.01	0.20 ± 0.02	0.39 ± 0.01
C18	1.22 ± 0.02a	1.85 ± 0.19b	2.90 ± 0.11c
C24	0.24 ± 0.02a	0.33 ± 0.04b	0.49 ± 0.02c
ΣSFA	**6.67 ± 0.15**	**9.54 ± 0.49**	**14.85 ± 0.20**
C15:1	0.16 ± 0.00a	0.17 ± 0.01a	0.21 ± 0.02b
C16:1	1.42 ± 0.19a	1.53 ± 0.09a	2.45 ± 0.10b
C17:1	0.23 ± 0.02	0.21 ± 0.02	0.34 ± 0.01
C18:1n9c	2.47 ± 0.13a	6.27 ± 0.20b	6.06 ± 0.18b
C18:1n7	1.68 ± 0.06	1.60 ± 0.04	1.55 ± 0.10
C20:1n9	0.44 ± 0.04	0.55 ± 0.08	0.92 ± 0.10
ΣMUFA	**6.23 ± 0.15**	**10.33 ± 0.24**	**11.62 ± 0.26**
C18:3n3 (ALA)	0.19 ± 0.01	0.26 ± 0.04	0.47 ± 0.06
C20:5n3 (EPA)	1.07 ± 0.13a	1.47 ± 0.10b	3.21 ± 0.09c
C22:5n3 (DPA)	0.28 ± 0.03	0.65 ± 0.07	1.43 ± 0.04
C22:6n3 (DHA)	1.42 ± 0.21a	3.67 ± 0.12b	8.84 ± 0.13c
Σω-3	**2.95 ± 0.25**	**5.79 ± 0.17**	**13.95 ± 0.17**
C18:2n6 (LA)	0.15 ± 0.01	0.22 ± 0.03	0.29 ± 0.01
C20:4n6 (AA)	0.47 ± 0.07a	0.99 ± 0.07b	1.31 ± 0.03c
Σω-6	**0.62 ± 0.07**	**1.21 ± 0.08**	**1.61 ± 0.04**
ΣPUFA	**3.58 ± 0.25**	**7.26 ± 0.20**	**15.56 ± 0.18**
Σω-3/Σω-6	4.8 ± 1.37	4.79 ± 0.94	8.69 ± 1.19
PUFA/SFA	0.54 ± 0.18	0.76 ± 0.31	1.05 ± 0.23
DHA/EPA	1.32 ± 0.25	2.50 ± 0.19	2.75 ± 0.09

4. Discussion

The present study assessed some biological aspects of *T. lyra*, namely age and growth, reproduction and chemical composition.

Regarding the length-frequency distribution, results showed that the length range sampled in the study was biased towards large individuals, with an absence of smaller ones. Olim and Borges (2006) obtained similar results when studying length-weight relationships for eight species of the family Triglidae in the South coast of Portugal. This may be explained by the fishing gear used (in the present study, trawls, trammel nets, traps and pots), as the sizes of fish caught is directly related with the characteristics of the fishing gear (Chopin and Arimoto, 1995). The mesh size used in the present study showed to be insufficient to catch smaller individuals, therefore explaining its lack in the sample. On the other hand, *T. lyra* is not a target species for the metier fishery, being mainly caught as an accessory species. Hence, some individuals could be rejected at sea including the ones with lower size, not being able to reach fish auctions and consequently being underrepresented or inexistent in the sample. Borges et al. (2001) studied discards of trawlers, seiners and trammel netters in the Algarve coast and reported that some species were discarded because they consisted of individuals that were too small. The absence of small individuals made it impossible to estimate other reproductive parameters such as length and age at first maturity in the present study.

The results also showed differences between both sexes in length-frequency distributions, with females reaching higher lengths than males. Mean TL was significantly different between sexes. This agrees with studies obtained for two other Triglidae species, by Marriott et al. (2010) for the red gurnard (*Chelidonichthys cuculus*) in Eastern Anglesey and Northwest Wales, and by Boudaya et al. (2008) for the tub gurnard (*Chelidonichthys lucerna*) in the Gulf of Gabès, Tunisia. Furthermore, the fact that males are smaller than females seems to be a common feature in triglids, and has previously been reported for *Chelidonichthys lucerna*, *Chelidonichthys lastoviza*, *Chelidonichthys cuculus* and *Eutrigla gurnardus* in Baie de Douarnenez (France) (Baron, 1985), and for *Chelidonichthys lucerna* in the Thermaikos Gulf (Greece) (Papaconstantinou, 1984).

Length-weight relationships are used to estimate the weight of a fish corresponding to a given length. These relationships are frequently used in different studies as indicators of overall growth and fish condition (Le Cren, 1951; Folkvord and Mosegaard, 2002;

Froese, 2006). Regarding length-weight relationship of *T. lyra*, the present study showed no significant differences between the growth of males and females. Similar results were obtained by Papaconstantinou (1981) for the Saronikos Gulf (Greece), and by Olim and Borges (2006) in the south coast of Portugal.

Furthermore, the outcomes of the present study indicated that the growth type of the species is isometric, because *b* was not significantly different from 3, which means that the fish grows without changing its shape (Le Cren, 1951; Folkvord and Mosegaard, 2002). On the other hand, Olim and Borges (2006) found that *T. lyra* exhibited positive allometric growth ($b > 3$), meaning that the fish changed its shape with increasing length. This may be explained by the fact that parameters of the length-weight relationship may vary significantly within species depending on season, population and environmental conditions (Moutopoulos and Stergiou, 2002; Froese, 2006). The fact that Olim and Borges (2006) used individuals ranging from 7 to 24 cm of TL while the present study used individuals ranging from 12.5 to 45.1 cm of TL, may also explain the differences in length-weight relationships and growth type obtained by both studies.

Regarding the choice of the method of preparation of the otoliths for age estimation of *T. lyra*, previous studies (Papaconstantinou, 1981; Papaconstantinou et al., 1992) used burned otoliths since this method seemed to increase the visibility of annual growth increments, as described by Pentilla and Dery (1988). However, in the present study, the process of burning caused the otoliths to crack, even using a lower temperature (200º) than that proposed by Papaconstantinou (1981) and Papaconstantinou et al. (1992) (450 ºC), and this might be a sign of overbaking. Moreover, whole otoliths showed a better differentiation and visibility of growth increments, leading to the choice of this method for systematic readings.

Concerning the determination of consistency of age determinations, Campana et al. (1995) recommend the use of a combination of methodologies. In the present study, age bias plots were constructed, and indices of precision were determined based on the reading of three readers. Age bias plots showed some deviation from the 1:1 equivalence line for ages greater than 5/6 years indicating some disagreement in age assignment between readers over these ages, and values of CV and APE were above the limits suggested by Campana (2001) (CV < 7.6 %, APE = 5.5 %). This can be related to the existence of a considerable number of large individuals with small otoliths, which was demonstrated by the relationship between body length and otolith radius ($R^2 = 0.6731$)

(Fig. 3.5). This fact, together with some discontinuities in the otolith, made it difficult to identify the *annuli* (especially in larger individuals) and to assign age to one individual, leading to the observed high values of the indices of precision. Lower values of APE indicate that greater precision in age estimation is achieved (Beamish and Fournier, 1981). In the present study, however, the results suggested some imprecision between readers, with the readings between readers 1 and 2 being the most precise and the readings between readers 2 and 3 being the least precise. In the future, the sample could be reinforced, with more otoliths being read. On the other hand, a different reading technique could be used, namely sectioning, as done for the tub gurnard (*Chelidonichthys lucerna*) (Boudaya et al., 2008).

In the present study, validation of the frequency of formation of growth increments was performed using the semi-direct validation methods of analysis of otolith edge type evolution throughout the year and analysis of marginal increment ratio (MIR). The results indicated a higher percentage of opaque edges in May (late Spring) and September (late Summer), and a higher percentage of translucent edges in November (late Autumn) and December (early Winter). Samples during Summer months were not obtained in this study, although the results suggested an increasing tendency in the percentage of opaque increments towards June, July and August, as well as higher values of MIR in those months. In fact, the highest values of MIR occurred in May and September, as well as the highest percentage of opaque increments. MIR and edge type analysis suggested that a single set of translucent and opaque increments is formed every year in *T. lyra* off the Portuguese continental coast. Translucent increments are deposited in Autumn/Winter (lower values of MIR) and opaque increments are formed in Spring/Summer (higher values of MIR). A single increment (composed of translucent and opaque) is probably completely formed in Summer (higher values of MIR). The fact that an upwelling occurs every year in west Iberian coast in Spring and Summer leading to a phytoplankton bloom, higher availability of food and higher growth of fish (Ambar and Dias, 2008), supports the complete deposition of an annual increment in Summer in *T. lyra*.

In terms of age estimation, the maximum age assigned for females was 12 years, while for males was 10 years. Differences in maximum age between sexes may be explained by different mortality rates between sexes, as suggested by Papaconstantinou (1986) for *Chelidonichthys lastoviza* whose females reached greater ages than males. Furthermore, for the Saronikos Gulf, the maximum age assigned to the population of *T. lyra* (including

females and males) was 7 years (Papaconstantinou, 1981), which can be related with the fact that it is a different habitat with different conditions comparing with the Portuguese coast.

To estimate the von Bertalanffy growth parameters of the piper gurnard, three different adjustment methods were used and the c-AIC indicated that back-calculation was the best method to estimate von Bertalanffy growth parameters, since it presented the lowest value. Nevertheless, the growth parameters estimated by this method indicate that $L\infty$ (42.579 cm) is lower than the maximum length sampled (45.1 cm). The difficulties found in age estimation, the lack of small individuals in the sample, the small sample sizes and the relationship between body length and otolith radius ($R^2 = 0.6731$) could justify these results. Improvement of the results could be done reinforcing the sample with smaller individuals, adjusting the methodological approach using digital tools to take more precise measurements of the otolith radius and increments, and redefining the reading protocols. A maximum total length of 57.438 cm for the Aegean Sea (Papaconstantinou et al., 1992) was estimated, revealing differences with the values obtained in the present work. These differences may be explained by different habitats, since fish growth depends on environmental factors (availability of food, temperature) (Magnussen, 2007) that vary between the Portuguese coast, Saronikos Gulf and Aegean Sea, but also with differences related with different ageing and reading protocols. Boudaya et al. (2008) obtained a $L\infty$ of 40.26 cm for males and a $L\infty$ of 46.16 cm for females of *Chelidonichthys lucerna* in the Gulf of Gabès (similar to the obtained in the present study) and k values of 0.06 and 0.05 for males and females, respectively, which, compared to the value obtained for *T. lyra* (0.204), suggested that *Chelidonichthys lucerna* could be a slow growing species. In turn, Papaconstantinou (1986) reported that *Chelidonichthys lastoviza* in Saronikos Gulf has a $L\infty$ of 35.6 cm, reaching lower lengths than *T. lyra*, and a k of 0.133, lower than the one obtained for *T. lyra*. Marriott et al. (2010) obtained 42.4 cm of $L\infty$ and 0.21 of k for *Chelidonichthys cuculus* in the Irish Sea, which are very similar to those determined for *T. lyra* in the present study. Given this, the estimated parameters obtained in the present research suggested that *T. lyra* grows in a similar rate to *Chelidonichthys cuculus*, faster than *Chelidonichthys lucerna* and slower than *Chelidonichthys lastoviza*.

Regarding the analysis of the sex ratio, a higher abundance of females in relation to males was verified in almost every month, particularly during the spawning season (November to February). Papaconstantinou (1981, 1992) observed a predominance of males in all

seasons of the year in Saronikos Gulf. However, for other triglids a predominance of females is also documented, namely in *Chelidonichthys lucerna* in the Gulf of Gabès (Boudaya et al., 2008) and in *Eutrigla gurnardus* in Greek Seas (Papaconstantinou, 1983).

Differences in the sex ratio may suggest sexual segregation, for example regarding habitat, meaning that females and males occur in different zones (Wearmouth and Sims, 2008) that are targeted differently by the fishery. Furthermore, the preponderance of females in the population may be explained by the sexual difference in growth (Qasim, 1966). Females attain greater lengths than males, which may be related to a higher longevity in females, explaining its higher abundance in the sampling. On the other hand, individuals with larger size (in this case, females) probably suffer less from predation and are also favoured in terms of intra and interspecific competition for food and space. Larger lengths seem to lead to higher probability of survival (Qasim, 1966), justifying the fact that in the present study sex ratio is biased towards females.

Concerning the structure of the gonads, *T. lyra* followed the type of organization that is typical of most teleost fish. The stages of development in male cells (spermatogonia, spermatocytes, spermatids, and spermatozoa) are common to most teleost fish (Grier, 1981; Nagahama, 1983), as well as the oocyte developmental stages (Grier, 1981; Nagahama, 1983, Lowerre-Barbieri et al., 2011). In terms of the diameter, female gametes, unlike male gametes (where spermatogonia are the largest cells), go through an increase in cell diameter throughout gametogenesis (Nagahama, 1983). As expected, the diameter of female sexual cells increased along oogenesis (from PG stage to H stage) due to the accumulation of yolk, while the diameter of male sexual cells decreased along spermatogenesis (from Sg stage to Sz stage). Muñoz et al. (2002) studied gonadal structure and gametogenesis of *T. lyra* in Costa Brava (Mediterranean) and obtained different results regarding the diameter of sexual cells. In females, the main difference is in the diameter of yolked oocytes, because the author distinguished only two stages of yolked oocytes, while in the present study three stages of yolked oocytes were identified. In males, the spermatozoids in the present study had larger diameter (2.4 μm) than spermatozoids in Costa Brava.

In the present study, spawning season of *T. lyra* was defined based on the monthly frequency of maturity phases of the reproductive cycle corroborated by the evolution of energetic indices along months. Actively spawning females occurred in the period between November 2018 and March 2019, with the highest percentage in January,

whereas spawning capable males appeared from September 2018 to October 2018 and from January 2019 to April 2019, with the highest percentage in January, February and April.

The highest values of female GSI occurred between November 2018 and March 2018, with a peak in January which corresponded to the month with highest percentage of AS females. Male GSI was higher in January 2019 and February 2019, when all males sampled were in SC phase. Throughout the months of sampling males showed lower values of GSI than females, which agrees with what is found for most fish species, as males do not need to spend as many resources as females in gamete production (Trivers, 1972). Female GSI and male GSI presented significant differences among months, specially between January 2019 and February 2019 and the other months, since during the spawning season there was a higher percentage of spawning capable individuals and the gonads were bigger, leading to higher values of GSI. Regarding the evolution of GSI throughout maturity phases, both male and female GSI presented the highest values in SC and AS phases, respectively, which was according to what was expected, as in that phases the weight of the gonads reaches its highest values. In general, the evolution of GSI corroborated the evolution of maturity phases.

As for the evolution of HSI and K throughout the year, significant differences were obtained between months for both sexes. It would be expected to have higher values of HSI and K before or at the beginning of the reproductive season, which is linked to an increase in the synthesis of lipids and proteins in the liver (Palazón-Fernández et al., 2001) and with the mobilization of hepatic and muscle reserves for reproduction, followed by lower values of HSI and K during the months of reproduction, as most of the energy is targeted to the gonads during reproduction (Le Cren, 1951). In fact, the liver plays a crucial role in reproduction, particularly in females, being responsible for the production of vitellogenin and eggshell proteins that are taken up by oocytes during vitellogenesis (Lubzens et al., 2010). In the present study, female HSI and K increased from May 2018 to January 2019, and then decreased. This was according to the expected and suggested that the fish accumulates energy reserves in the muscle and liver during the months before the peak of spawning (January), and as the energy is being channelled to the gonad the HSI and K decrease. Regarding the evolution of male HSI and K, the highest values were verified in September 2018 (corresponding to the appearance of spawning capable males) followed by a decreasing tendency until May 2019, which was also according to the

expected. Males invest in feeding as well as in the accumulation of lipids and proteins in the liver and muscle before reproducing, followed by a decrease in the reserves as they are being targeted to the gonad. Furthermore, in terms of the evolution of HSI and K throughout maturity phases, values of HSI were higher in SC females and De males, while values of K were higher in AS females and De males, which preceded or coincided with the beginning of spawning. So, the evolution of HSI and K also corroborated the evolution of maturity phases in *T. lyra*.

Given the monthly percentage of maturity phases and the monthly evolution of indices, spawning season of *T. lyra* was defined as the period between November and February, indicating that the species has a relatively short spawning season. Different spawning seasons were reported for the Aegean Sea (Papaconstantinou et al., 1992), where spawning is considered to take place in Summer, and for the Greek Seas (Papaconstantinou, 1983) and Costa Brava (Mediterranean Sea) (Muñoz et al., 2002), where the reproduction period occurs from September to March.

Water temperature is one of the most important factors influencing spawning seasonality and timing of gametogenesis in fish (Lam, 1983; Pankhurst and Porter, 2003; Lowerre-Barbieri et al., 2011b), with some species reproducing in warmer months (*Serranus atricauda*, Neves et al., 2009; *Scomber scombrus*, Borja et al., 2002) and others in colder months of the year (*Sardina pilchardus*, Stratoudakis et al., 2007; *Helicolenus dactylopterus*, Sequeira et al., 2012), in Portuguese waters. Other important factors determining when a species should reproduce are photoperiod (Bye, 1990; Bromage et al., 2001), salinity (Lam, 1983), rainfall and social interactions (Lowerre-Barbieri, 2011b). All these environmental factors assure that spawning occurs at the appropriate time and when the conditions are more suitable for offspring survival. In the case of *T. lyra*, it seems that spawning takes place in different times of the year in different regions (Portuguese coast, Aegean Sea and Costa Brava), which may be explained by different conditions and environmental factors operating in those regions, influencing spawning seasonality.

Regarding *T. lyra* type of fecundity, the results indicated the presence of a hiatus between the unyolked oocytes and the yolked/mature oocytes and an increase in the percentage of yolked and mature oocytes from the developing phase to the actively spawning phase followed by a decrease in the regressing phase. Furthermore, the results indicated a decline of the number of Vtg3 and an increase in the mean diameter of Vtg3 along the

spawning season, and no massive atresia occurring at the end of the spawning season, suggesting determinate fecundity for *T. lyra*. Fish species with this type of fecundity are also characterized by short reproductive seasons (Hickling and Rutenberg, 1936), as the case of the black scabbardfish (*Aphanopus carbo*) (Neves et al., 2009), the European bass (Mayer et al., 1990), the Atlantic cod (*Gadus morhua*) (Thorsen et al., 2010) and *T. lyra* off the portuguese coast, supporting once more determinate fecundity for this species.

Although no previous studies on *T. lyra* fecundity are available for comparison purposes, this biological parameter is being investigated for the red gurnard (Chelidonichthys cuculus, Triglidae family) under the VALOREJET project. The preliminary results indicate indeterminate fecundity for this species, which to be true constitutes a curiosity as two close species that share the same habitat show different fecundity strategies. This is not unique since it has already been reported for other species such as Atlantic mackerel (*Scomber scombrus*) and chub mackerel (*Scomber japonicus*), with the former seeming to have determinate fecundity (Greer Walker et al., 1994) and the latter exhibiting indeterminate fecundity (Dickerson et al., 1992; Murua and Saborido-Rey, 2003).

Although estimation of fecundity was not performed in the present study it would be assessed in future studies. The determination of the fecundity type is the first step to choose the best methodology to follow to estimate fecundity. In species with determinate fecundity, as is the case of *T. lyra*, there are some aspects to be considered when estimating fecundity. First, when estimating total fecundity, atretic losses must be discounted from potential annual fecundity since fecundity is fixed before the beginning of spawning (Hunter et al., 1992; Murua et al., 2003). Secondly, it is important that sampling covers the period before and during spawning to guarantee that fecundity is assessed for the entire stock (Murua et al., 2003). Moreover, another important aspect when estimating fecundity is that females to be chosen cannot show the presence of postovulatory follicles (POFs) or hydrated oocytes in the ovaries because its presence indicate that the individual has already begun the spawning process (Murua et al., 2003), and histological procedures are crucial to confirm this aspect. Different methods can be used in estimating fecundity, but most approaches involve taking ovarian subsamples and the application of the gravimetric method (Murua et al., 2003; Ganias et al., 2014).

The reproduction study developed in the present work allowed to define *T. lyra* reproductive strategy. In terms of gender system, *T. lyra* is gonochoristic because it presented separation of sexes, with sex being fixed at maturation. With respect to the type

of fertilization, it is external, and the embryos developed outside the ovaries. Oocyte development in *T. lyra* is group-synchronous, as not all development stages of oocytes were always present during the spawning season. At any time in the ovary, there was a group of smaller oocytes including PG and CA oocytes, and a group of larger oocytes that developed over time to be spawned. This feature was already reported for this species in Costa Brava in the Mediterranean Sea (Muñoz et al., 2002). This type of oocyte development, where different populations of oocytes with synchronous development can be distinguished at any time in the ovary (Wallace and Selman, 1981), is common in iteroparous species with short spawning seasons (Murua and Saborido-Rey, 2003), as is the case of *T. lyra*. Lastly, the histological analysis of the gonads indicated that the species is a batch spawner, once advanced yolked oocytes (Vtg3) appeared at the same time as hydrated oocytes in some females in actively spawning phase. This indicated the release of different batches at different times during the spawning season. Such type of spawning is common in many other species of temperate and cold environments of the Atlantic (Murua and Saborido-Rey, 2003).

Regarding the chemical composition of the muscle of *T. lyra*, the results obtained showed that, in general, throughout the months of sampling, moisture was higher compared to levels of ash content, protein content and total fat. The results were according to what was expected, as water is the major component in fish muscle, followed by proteins (Huss, 1995; Murray and Burt, 2001; Nunes et al., 2011). However, ash content (representing minerals), which usually represents a residual part of the composition of fish (between 1 and 2 %) (Huss, 1995; Murray and Burt, 2001), reached higher values than total fat in the present study. This indicates that *T. lyra* is a good source of minerals for human health, including possibly iodine and selenium which are major constituents of seafood (Nunes et al., 2011).

Values of total fat in the muscle ranged between 1.73 % in January and 0.74 % in March, suggesting that the species is lean (presents low fat content) (Nunes et al., 2011). Similar results were obtained for *T. lyra* in the Mediterranean Sea, where total lipid content in the muscle was found to be 0.66 % of the wet tissue (Loukas et al., 2010). In terms of the influence of different months in total fat content, in the present work there were significant differences among months. The highest value was verified in January (winter) which can be related to the fact that *T. lyra* was reproducing during that month (corresponding to the peak of spawning), being necessary high concentrations of lipids to

help in the development of the oocytes (Lubzens et al., 2010). Furthermore, in January it was verified the highest value of HSI in females, which can be linked to an increase in the synthesis of lipids in the liver (Palazón-Fernández et al., 2001).

Protein content in the muscle of *T. lyra* ranged between 16.55 % in January and 17.65 % in March. This agreed with the results obtained for most seafood species, that vary between 10 and 25 % (Nunes et al., 2011). In terms of the influence of different months in protein content, significant differences were found among months. A previous study on the chemical composition of the tub gurnard (*Chelidonichthys lucerna*) in the Adriatic Sea (Roncarati et al., 2014) reported a protein content of approximately 19 %, which is similar to the values obtained in this work.

A total of 21 fatty acids were identified in *T. lyra* muscle, contrary to the 18 fatty acids found in *T. lyra* in the Mediterranean Sea (Loukas et al., 2010), which can be related with different methodological protocols applied. Within the group of SFAs, palmitic acid (C16) was the most abundant, and within the group of MUFAs, oleic acid (C18:1n9c) was the predominant fatty acid. Amongst PUFAs, ω-3 fatty acids presented the highest concentrations, namely docosahexaenoic acid (DHA) (highest concentration) and eicosapentaenoic acid (EPA). Similar outcomes were obtained by Loukas et al. (2010) for *T. lyra* in the Mediterranean, as well as for most fish species (Nunes et al., 2003, 2011). The results indicate a PUFA/SFA ratio between 0.54 and 1.05, a DHA/EPA ratio between 1.32 and 2.75, and a ω-3/ω-6 ratio between 4.8 and 8.69, which were similar to the values obtained by Loukas et al. (2010) and suggested that *T. lyra* is a good source of the mentioned components. These ratios, together with EPA and DHA contents, give important information on the benefits to human health of consuming a certain species (Loukas et al., 2010; Nunes et al., 2011).

The composition of *T. lyra* muscle in some fatty acids varied between months. In May 2019, *T. lyra* muscle presented the highest quantity of fatty acids, which may be explained by a higher availability of phytoplankton in the environment, a source of fatty acids namely long-chain ω-3 PUFAs that are accumulated through the marine food chain and reach *T. lyra* organism through feeding (Loukas et al., 2010). An upwelling regime occurs in the west Iberian coast in Spring and Summer, bringing new nutrients into the photic zone and allowing higher availability of phytoplankton during that period (Ambar and Dias, 2008). This may be linked to the increase in the quantity of fatty acids in *T. lyra*

muscle from January, when phytoplankton availability is low, to May, when there is high availability of phytoplankton.

5. Conclusions

The present work aimed to improve the knowledge on some life history parameters of *T. lyra*, namely age and growth and reproduction, as well as to study chemical composition of the muscle, and in this way evaluate the potential of valorisation of a species with a low commercial value in Portugal.

Concerning the study of age and growth, otolith reading revealed to be a demanding process, which involved a period of adaptation to the interpretation of these calcified structure and awareness with the method of counting the annual growth increments. The results obtained stand out the isometric growth of the species, the deposition of a single set of translucent and opaque increments every year, and a longevity of 12 years for *T. lyra* off the Portuguese continental coast. In the future, it would be interesting to test otolith sectioning to evaluate its adequacy in improving visibility of growth increments and obtain more reliable age estimation, to reinforce the sample with smaller individuals, to redefine the reading protocols, to adjust the methodological approach using digital tools to take more precise measurements of the otolith radius and nucleus-to-increment distances, improving the relationship between fish body length and otolith radius and the adjustment of the back-calculation method. These procedures could help to improve the results on *T. lyra* age and growth.

In terms of reproduction, the identification of the different stages of development of oocytes and germ male cells as well as histological staging of the gonads improved with time and experience, allowing to reach some conclusions about the reproductive strategy of the species. The results highlighted that *T. lyra* spawns between November and February, a relatively short period that is usually typical of species with determinate fecundity, which proved to be the case after the analysis of the fecundity type performed for the first time under the present study. Moreover, the outcomes suggest a group-synchronous oocyte development and batch spawning for *T. lyra*. The results obtained in this study allow future fecundity estimation and the choice of the best method to do it. Based on the spawning season of *T. lyra*, fisherman should try to avoid overfishing during January and February, when most individuals are spawning.

Regarding the chemical composition of *T. lyra* muscle, the main constituent was water, followed by proteins, minerals (ash) and lipids. Fatty acid composition showed high concentrations of PUFAs, namely ω-3 fatty acids including docosahexaenoic acid (DHA)

and eicosapentaenoic acid (EPA), which are highly beneficial to human health. Thus, *T. lyra* displays good nutritional characteristics and constitute a valuable resource for human consumption. From a nutritional point of view, and with the results already available, the best period to fish the piper gurnard seems to be May, since it presents the highest concentrations of fatty acids, including DHA and EPA, as well as the highest mineral content.

Concluding, the present study contributed to an improvement of the knowledge of life history parameters of *T. lyra*, namely of age and growth and reproduction, which constitute essential information for the management of the species exploration in Portugal. The analysis of the chemical composition of the species allowed to know its nutritional characteristics and, thus, to advance in the future valorisation of the species as a fishing resource, for example through a better use of the resource and creation of new products for consumption, which can be important, since *T. lyra* is a species with low commercial value in Portugal.

6. References

Alonso-Fernández, A., Domínguez-Petit, R., Bao, M., Rivas, C., Saborido-Rey, F. 2008. Spawning pattern and reproductive strategy of female pouting *Trisopterus luscus* (Gadidae) on the Galician shelf of north-western Spain. Aquatic Living Resources, 21: 383-393.

Alverson, D.L., Freeberg, M.H., Murawski, S.A., Pope, J.G. 1994. A global assessment of fisheries bycatch and discards. FAO, Fisheries Technical Paper, 339.

Ambar, I., Dias, J. 2008. Remote sensing of coastal upwelling in the North-Eastern Atlantic Ocean. In Remote sensing of the European seas, 141-152. Springer, Dordrecht, Netherlands.

Assis, C.A.D.S. 2000. Estudo morfológico dos otólitos Sagitta, Asteriscus e Lapillus de teleósteos (Actinopterygii, teleostei) de Portugal Continental. Dissertação para obtenção do grau de Doutor em Biologia, na especialidade de Ecologia e Biossistemática. Faculdade de Ciências da Universidade de Lisboa, Lisboa, Portugal.

Baron, J. 1985. Les Triglides (Teleosteens, Scorpaeniformes) de la Baie de Douarnenez. La croissance de *Eutrigla gurnardus*, *Trigla lucerna*, *Trigloporus lastoviza* et *Aspitrigla cuculus*. Cybium 9: 127-144.

Beamish, R.J., Fournier, D.A. 1981. A method for comparing the precision of a set of age determinations. Canadian Journal of Fisheries and Aquatic Sciences, 38: 982-983.

Bellido, J.M., Santos, M.B., Pennino, M.G., Valeiras, X., Pierce, G.J. 2011. Fishery discards and bycatch: solutions for an ecosystem approach to fisheries management? Hydrobiologia, 670: 317-333.

Bligh, E.G., Dyer, W.J. 1959. A rapid method of total lipid extraction and purification. Canadian journal of biochemistry and physiology, 37: 911-917.

Borges, L. 2015. The evolution of a discard policy in Europe. Fish and Fisheries, 16: 534-540.

Borges, T.C., Erzini, K., Bentes, L., Costa, M.E., Gonçalves, J.M.S., Lino, P.G., Ribeiro, J. 2001. By-catch and discarding practices in five Algarve (southern Portugal) métiers. Journal of Applied Ichthyology, 17: 104-114.

Boudaya, L., Neifar, L., Rizzo, P., Badalucco, C., Bouain, A., Fiorentino, F. 2008. Growth and reproduction of *Chelidonichthys lucerna* (Linnaeus) (Pisces: Triglidae) in the gulf of Gabès, Tunisia. Journal of Applied Ichthyology, 24: 581-588.

Borja, A., Uriarte, A., Egana, J. 2002. Environmental factors and recruitment of mackerel, *Scomber scombrus* L. 1758, along the North-east Atlantic coasts of Europe. Fisheries Oceanography, 11: 116–127.

Bromage, N., Porter, M., Randall, C. 2001. The environmental regulation of maturation in farmed finfish with special reference to the role of photoperiod and melatonin. Aquaculture, 197: 63-98.

Brown-Peterson, N.J., Wyanski, D.M., Saborido-Rey, F., Macewicz, B.J., Lowerre-Barbieri, S.K. 2011. A standardized terminology for describing reproductive development in fishes. Marine and Coastal Fisheries, 3: 52-70.

Bye, V.J. 1990. Temperate marine teleosts. In Reproductive seasonality in teleosts: environmental influences actors controlling reproductive seasonality in temperate water fish. Edition by Munro, A.D., Scott, A.P., Lam, T.J. CRC Press, Inc., Boca Raton, Florida, USA.

Campana, S.E. 2001. Accuracy, precision and quality control in age determination, including a review of the use and abuse of age validation methods. Journal of Fish Biology, 59: 197-242.

Campana, S.E., Jones, C.M. 1992. Analysis of otolith microstructure data. Otolith microstructure examination and analysis. Canadian Special Publication of Fisheries and Aquatic Sciences, 117: 73-100.

Campana, S.E., Annand, M.C., McMillan, J.I. 1995. Graphical and statistical methods for determining the consistency of age determinations. Transactions of the American Fisheries Society, 124: 131-138.

Caragitsou, E., Papaconstantinou, C. 1994. Feeding habits of piper (*Trigla lyra*) in the Saronikos Gulf (Greece). Journal of Applied Ichthyology, 10: 104-113.

Chang, W.Y.B. 1982. A statistical method for evaluating the reproducibility of age determination. Canadian Journal of Fisheries and Aquatic Sciences, 39: 1208-1210.

Chopin, F.S., Arimoto, T. 1995. The condition of fish escaping from fishing gears - a review. Fisheries research, 21: 315-327.

Clucas, I. 1997. A study of the options for utilization of bycatch and discards from marine capture fisheries. FAO Fisheries Circular, 928: 1-59.

Dickerson, T.L., Macewicz, B.J., Hunter, J.R. 1992. Spawning frequency and batch fecundity of chub mackerel, *Scomber japonicus*, during 1985. California Cooperative Oceanic Fish Investigations Reports, 33: 130-140.

Domínguez-Petit, R., Anastasopoulou, A., Cubillos, L., Gerritsen, H.D., Gonçalves, P., Hidalgo, M., Kennedy, J., Korta, M., Marteinsdottir, G., Morgado, C., Muñoz, M.,Quincoces, I., Saínza, M., Thorsen, A., Vitale, F. 2017. Chapter 3: maturity. In Handbook of applied fisheries reproductive biology for stock assessment and management. Edition by Domínguez-Petit, R., Murua, H., Saborido-Rey, F., Trippel, E. Digital CSIC, Vigo, Spain.

EU. European Council Regulation No 1380/2013 of the European Parliament and of the Council of 11 December 2013 on the Common Fisheries Policy, amending Council Regulations EC No 1954/2003 and EC No 1224/2009 and repealing Council Regulations EC No 2371/2002 and EC No 639/2004 and Council Decision 2004/585/EC. Off. J. Eur. Union 2013, L354, 22-61. https://eur-lex.europa.eu/legal-content/EN/TXT/?uri=celex%3A32013R1380

Fernández, A., Grienke, U., Soler-Vila, A., Guihéneuf, F., Stengel, D.B., Tasdemir, D. 2015. Seasonal and geographical variations in the biochemical composition of the blue mussel (*Mytilus edulis* L.) from Ireland. Food chemistry, 177: 43-52.

Fischer, W., Bauchot, M.L., Schneider, M. 1987. Guide FAO d'identification des espèces pour les besoins de la pêche. Méditerranée et mer Noire - Zone de Pêche 37. Volume 2. FAO, Rome, Italy.

Folch, J., Lees, M., Sloane, S.G.H. 1957. A simple method for the isolation and purification of total lipides from animal tissues. Journal of Biological Chemistry, 226: 497-509.

Folkvord, A., Mosegaard, H. 2002. Chapter V-A: growth and growth analysis. In Manual of fish sclerochronology. Edition by Panfili, J., Pontual, H. (de), Troadec, H., Wright, P.J. Ifremer-IRD coedition. Brest, France.

Francis, R.I.C.C. 1990. Back-calculation of fish length: a critical review. Journal of Fish Biology, 36: 883-902.

Froese, R. 2006. Cube law, condition factor and weight–length relationships: history, meta-analysis and recommendations. Journal of Applied Ichthyology, 22: 241-253.

Ganias, K., Murua, H., Claramunt, G., Dominguez-Petit, R., Gonçalves, P., Juanes, F., Keneddy, J., Klibansky, N., Korta, M., Kurita, Y., Lowerre-Barbieri, S., Macchi, G., Matsuyama, M., Medina, A., Nunes, C., Plaza, G., Rideout, R., Somarakis, S., Thorsen, A., Uriarte, A., Yoneda, M. 2014. Chapter 4: egg production. In Handbook of applied fisheries reproductive biology for stock assessment and management. Edition by Domínguez-Petit, R., Murua, H., Saborido-Rey, F., Trippel, E. Digital CSIC, Vigo, Spain.

Gordo, L.S., Neves, A., Vieira, A.R., Paiva, R.B., Sequeira, V. 2016. Age, growth and mortality of the comber *Serranus cabrilla* (Linnaeus, 1758) in the Eastern Atlantic. Marine Biology Research, 12: 656-662.

Greer Walker, M., Witthames, P.R., Bautista De Los Santos, I. 1994. Is the fecundity of the Atlantic mackerel (*Scomber scombrus*: Scombridae) determinate? Sarsia, 79: 13-26.

Grier, H.J. 1981. Cellular organization of the testis and spermatogenesis in fishes. American Zoologist, 21: 345-357.

Guillen, J., Holmes, S.J., Carvalho, N., Casey, J., Dörner, H., Gibin, M., Zanzi, A. 2018. A review of the European union landing obligation focusing on its implications for fisheries and the environment. Sustainability, 10: 900-912.

Hall, M.A. 1996. On bycatches. Reviews in Fish Biology and Fisheries, 6: 319-352.

Hall, M.A., Alverson, D.L., Metuzals, K.I. 2000. Bycatch: problems and solutions. Marine Pollution Bulletin, 41: 204-219.

Hall, S.J., Mainprize, B.M. 2005. Managing by-catch and discards: how much progress are we making and how can we do better? Fish and Fisheries, 6: 134-155.

Hickling, C.F., Rutenberg, E. 1936. The ovary as an indicator of the spawning period in fishes. Journal of the Marine Biological Association of the United Kingdom, 21: 311-317.

Hill, B.J., Wassenberg, T.J. 1990. Fate of discards from prawn trawlers in Torres Strait. Marine and Freshwater Research, 41: 53-64.

Holden, M.J., Raitt, D.F.S. 1974. Manual of fisheries science: 5 - Sex, maturity and fecundity. FAO, Fisheries Technical Paper, 115.

Hunter, J.R., Macewicz, B.J., Chyan-huei Lo, N., Kimbrell, C.A. 1992. Fecundity, spawning, and maturity of female dover sole *Microstomus pacificus*, with an evaluation of assumptions and precision. Fishery Bulletin, 90: 101-128.

Huss, H.H. 1995. Quality and quality changes in fresh fish. FAO, Fisheries Technical Paper, 348.

ICES 2012. Report of the ICES Advisory Committee 2012. ICES Advice, 2012. Book 9, Section 9.4.24. International Council for the Exploration of the Sea, Copenhagen, Denmark.

Içemer, A., Özaydin, O., Benli, H.A., Katagan, T. 2002. Feeding habits of piper, *Trigla lyra* (Linnaeus, 1758) inhabiting the Aegean Sea. Acta Adriatica, 43: 77-82.

Jones, C.M. 2000. Fitting growth curves to retrospective size-at-age data. Fisheries Research, 46:123-129.

Kalish, J.M., Beamish, R.J., Brothers, E.B., Casselman, J.M., Francis, R.I.C.C., Mosegaard, H., Panfili, J., Prince, E.D., Thresher, R.E., Wilson, C.A., Wright, P.J. 1995. Glossary for otolith studies. In Recent developments in fish otolith research. Edition by Secor, D.H., Dean, J.M., Campana, S.E., Miller, A.B. University of South Carolina Press, Columbia, South Carolina, USA.

Kelleher, K. 2005. Discards in the world's marine fisheries: an update. FAO, Fisheries Technical Paper, 470.

Kjeldahl, J.Z. 1883. A new method for the determination of nitrogen in organic bodies. Analytical Chemistry, 22: 366-382.

Lam, T.J. 1983. Chapter 2: environmental influences on gonadal activity in fish. In Fish physiology: reproduction—behaviour and fertility control, volume 9B. Edition by Hoar, W.S., Randall, D.J., Donaldson, E.M. Academic Press, Cambridge, Massachusetts, USA.

Le Cren, E.D. 1951. The length-weight relationship and seasonal cycle in gonad weight and condition in the perch (*Perca flavescens*). Journal of Animal Ecology, 20:201-219.

Loukas, V., Dimizas, C., Sinanoglou, V.J., Miniadis-Meimaroglou, S. 2010. EPA, DHA, cholesterol and phospholipid content in *Pagrus pagrus* (cultured and wild), *Trachinus draco* and *Trigla lyra* from Mediterranean Sea. Chemistry and Physics of Lipids, 163: 292-299.

Lowerre-Barbieri, S.K., Brown-Peterson, N.J., Murua, H., Tomkiewicz, J., Wyanski, D.M., Saborido-Rey, F. 2011a. Emerging issues and methodological advances in fisheries reproductive biology. Marine and Coastal Fisheries, 3: 32-51.

Lowerre-Barbieri, S.K., Ganias, K., Saborido-Rey, F., Murua, H., Hunter, J.R. 2011b. Reproductive timing in marine fishes: variability, temporal scales, and methods. Marine and Coastal Fisheries, 3: 71-91.

Lubzens, E., Young, G., Bobe, J., Cerdà, J. 2010. Oogenesis in teleosts: how fish eggs are formed. General and Comparative Endocrinology, 165: 367-389.

Magnussen, E. 2007. Interpopulation comparison of growth patterns of 14 fish species on Faroe Bank: are all fishes on the bank fast-growing? Journal of Fish Biology, 71: 453-475.

Marriott, A.L., Latchford, J.W., McCarthy, I.D. 2010. Population biology of the red gurnard (*Aspitrigla cuculus* L.; Triglidae) in the inshore waters of Eastern Anglesey and Northwest Wales. Journal of Applied Ichthyology, 26: 504-512.

Mayer, I., Shackley, S.E., Witthames, P.R. 1990. Aspects of the reproductive biology of the bass, *Dicentrarchus labrax* L. II. Fecundity and pattern of oocyte development. Journal of Fish Biology, 36: 141-148.

Moutopoulos, D.K., Stergiou, K.I. 2002. Length–weight and length–length relationships of fish species from the Aegean Sea (Greece). Journal of Applied Ichthyology, 18: 200-203.

Muñoz, M., Sàbat, M., Mallol, S., Casadevall, M. 2002. Gonadal structure and gametogenesis of *Trigla lyra* (Pisces: Triglidae). Zoological Studies, 41: 412-420.

Murray, J., Burt, J.R. 2001. The composition of fish. Ministry of Technology, Torry Research Station, Torry Advisory Note, 38.

Murua, H., Kraus, G., Saborido-Rey, F., Witthames, P.R., Thorsen, A., Junquera, S. 2003. Procedures to estimate fecundity of marine fish species in relation to their reproductive strategy. Journal of Northwest Atlantic Fishery Science, 33: 33-54.

Murua, H., Saborido-Rey, F. 2003. Female reproductive strategies of marine fish species of the North Atlantic. Journal of Northwest Atlantic Fishery Science, 33: 23-31.

Nagahama, Y. 1983. Chapter 6: the functional morphology of teleost gonads. In Fish physiology, volume 9A. Edition by Hoar, W.S., Randall, D.J., Donaldson, E.M. Academic Press, Cambridge, Massachusetts, USA.

Nellemann, C., MacDevette, M., Manders, T., Eickhout, B., Svihus, B., Prins, A.G., Kaltenborn, B.P. 2009. The environmental food crisis – the environment's role in averting future food crises. A UNEP rapid response assessment. United Nations Environment Programme, GRID-Arendal, 23-24.

Neves, A., Vieira, A.R., Farias, I., Sequeira, V., Figueiredo, I., Gordo, L.S. 2009. Reproductive strategies in black scabbardfish (*Aphanopus carbo* Lowe, 1839) from the NE Atlantic. Scientia Marina, 73: 19-31.

Nunes, M.L., Bandarra, N.M., Batista, I. 2003. Fish products: contribution for a healthy food. Electronic Journal of Environmental, Agricultural and Food Chemistry, 2: 453-457.

Nunes, M.L., Bandarra, N.M., Batista, I. 2011. Health benefits associated with seafood consumption. In Handbook of Seafood Quality, Safety and Health Applications. Edition by Alasalvar, C., Shahidi, F., Miyashita, K., Wanasundara, U. Blackwell Science, Oxford, UK.

Olim, S., Borges, T.C. 2006. Weight–length relationships for eight species of the family Triglidae discarded on the south coast of Portugal. Journal of Applied Ichthyology, 22: 257-259.

Palazón-Fernández, J.L., Arias, A.M., Sarasquete, C. 2001. Aspects of the reproductive biology of the toadfish, *Halobatrachus didactylus* (Schneider, 1801) (Pisces: Batrachoididae). Scientia Marina, 65: 131-138.

Panfili, J. 2002. Chapter VIII-B: extraction and conservation of calcified structures. In Manual of fish sclerochronology. Edition by Panfili, J., Pontual, H. (de), Troadec, H., Wright, P.J. Ifremer-IRD coedition. Brest, France.

Pankhurst, N.W., Porter, M.J.R. 2003. Cold and dark or warm and light: variations on the theme of environmental control of reproduction. Fish Physiology and Biochemistry, 28: 385-389.

Papaconstantinou, C. 1981. Age and growth of piper, *Trigla lyra*, in Saronikos Gulf (Greece). Cybium, 5: 73-87.

Papaconstantinou, C. 1983. Observations on the ecology of gurnards (Pisces, Triglidae) of the Greek seas. Cybium, 7, 71-88.

Papaconstantinou, C. 1984. Age and growth of the yellow gurnard (*Trigla lucerna* L. 1758) from the Thermaikos Gulf (Greece) with some comments on its biology. Fisheries research, 2: 243-255.

Papaconstantinou, C. 1986. The life history of rock gurnard (*Trigloporus lastoviza*, Brünn. 1768) in the Saronikos Gulf. Journal of Applied Ichthyology, 2: 75-86.

Papaconstantinou, C., Petrakis, G., Caragitsou, E., Mytilineou, C. 1992. Preliminary study on the biology of piper (*Trigla lyra*, L. 1758) in the Aegean Sea. FAO, Fisheries Report, 477: 127-137.

Papaconstantinou, C., Farrugio, H. 2000. Fisheries in the Mediterranean. Mediterranean Marine Science, 1: 5-18.

Pentilla, J., Dery, L.M. 1988. Age determination methods for Northwest Atlantic species. NOAA Technical Report NMFS 72: 1-135.

Portuguese Institute of Quality 1988. Fishery - Determination of ash content, NP 2032.

Portuguese Institute of Quality 1991. Fish and fishing products - Determination of the water content, reference method. NP 2282.

Qasim, S.Z. 1956. Time and Duration of the Spawning Season in some Marine Teleosts in Relation to their Distribution. Extrait Du Journal Du Conseil International Pour L'exploration De La Mer, 21: 141-155.

Qasim, S.Z. 1966. Sex-ratio in fish populations as a function of sexual difference in growth rate. Current Science, 35: 140-142.

Ricker, W.E. 1973. Linear regressions in fishery research. Journal of the Fisheries Research Board of Canada, 30: 409-434.

Roncarati, A., Felici, A., Mariotti, F., Melotti, P. 2014. Flesh qualitative traits of tub gurnard (*Chelidonichthys lucerna* L.), a promising species candidate for aquaculture, captured in the middle Adriatic Sea in different seasons. Italian Journal of Animal Science, 13: 31-59.

Samamé, M. 1977. Determinación de la edad y crecimiento de la sardina *Sardinops sagax* sagax (J). Boletín-Instituto del Mar del Perú, 3:95-112.

Sequeira, V., Neves, A., Paiva, R.B., de Lima, J.P., Vieira, A.R., Gordo, L.S. 2012. Life history parameters as possible discriminators of bluemouth *Helicolenus dactylopterus* (Delaroche, 1809) populations in Portuguese waters. Fisheries Research, 125-126: 69-76.

Shono, H. 2000. Efficiency of the finite correction of akaike's information criteria. Fisheries Science, 66: 608-610.

Statistics Portugal 2018. Statistical data for Fisheries: 2007-2017. https://ine.pt/xportal/xmain?xpid=INE&xpgid=ine_indicadores&indOcorrCod=0001073&contexto=bd&selTab=tab2. Accessed in 14 December, 2018.

Stratoudakis, Y., Coombs, S., de Lanzós, A.L., Halliday, N., Costas, G., Caneco, B., Silva, A., Bernal, M. 2007. Sardine (*Sardina pilchardus*) spawning seasonality in European waters of the Northeast Atlantic. Marine Biology, 152: 201-212.

Thorsen, A., Witthames, P.R., Marteinsdóttir, G., Nash, R.D.M., Kjesbu, O.S. 2010. Fecundity and growth of Atlantic cod (Gadus morhua L.) along a latitudinal gradient. Fisheries Research, 104: 45–55.

Trivers, R.L. 1972. Parental investment and sexual selection. In Sexual selection and the descent of man. Edition by Campbell, B. Aldine-Atherton, Chicago, Illinois, USA.

von Bertalanffy, L. 1938. A quantitative theory of organic growth (inquiries of growth laws II). Human Biology, 10: 181-213.

Wallace, R.A., Selman, K. 1981. Cellular and dynamic aspects of oocyte growth in teleosts. American Zoologist, 21: 325-343.

Wearmouth, V.J., Sims, D.W. 2008. Sexual segregation in marine fish, reptiles, birds and mammals: behaviour patterns, mechanisms and conservation implications. Advances in Marine Biology, 54: 107-170.

Wilson, J.A., Vigliola, L., Meekan, M.G. 2009. The back-calculation of size and growth from otoliths: validation and comparison of models at an individual level. Journal of Experimental Marine Biology and Ecology, 368: 9-21.

Whitehead, P. J. P., Bauchot, M. L., Hureau, J. C., Nielsen, J., Tortonese, E. 1986. Fishes of the North-eastern Atlantic and the Mediterranean. Volume 3. Unesco. Paris, France.

Wright, P.J., Panfili, J., Morales-Nin, B., Geffen, A.J. 2002. Chapter II-A: otoliths. In Manual of fish sclerochronology. Edition by Panfili, J., Pontual, H. (de), Troadec, H., Wright, P.J. Ifremer-IRD coedition. Brest, France.

Zar, J.H. 1999. Biostatistical Analysis. Prentice-Hall, Inc, New Jersey, USA.

7. Appendix

Protocol for histological preparation of gonads

A. Fixation

1. After being removed from the abdominal cavity of fish, gonads are fixed in 4% buffered formalin and stored in plastic tubes for one month.
2. After being removed from formalin solution, transverse sections of the gonads are cut with a scalpel and placed in plastic tubes.
3. Then, the sections are de-hydrated with alcohol at different concentrations and different periods according to the following steps:
   i. From one day to the following (or 1 hour) in alcohol 70%
   ii. 30 min in alcohol 70%
   iii. 45 min in alcohol 90%
   iv. 45 min in alcohol 90%
   v. 1 hour in alcohol 96%
   vi. 1 hour in alcohol 96%
   vii. 1 hour in alcohol 96%
   viii. From one day to the following, in a 50 % solution of half alcohol 96% + pure resin (clean the gonads with absorbent paper and close the tubes)
   ix. 24 hours in pure resin (change the gonads to other plastic tubes)

Preparation of the solution of pure resin:

- Join a package of resin to 100 ml of resin in a flask;
- Put in the magnetic agitator with a magnet during 30 min;
- Store in the fridge, covered with parafilm, until later using.

B. Assembly

1. After removing gonad sections from the plastic tubes, put them in molds for the blocks of resin and fill the mold with a mixture of resin and a hardener (15 ml of pure resin + 1 ml of hardener) so that the section is completely covered.
2. Heat at a temperature of 50 ºC until the portions of gonad are solidified.
3. Leave it drying for 48 hours (or more) in horizontal position (if necessary, put weights above the cuvets).

C. Cut

1. After the blocks of resin are well dried and solidified, remove them from the molds and glue them to small wood blocks
2. Leave it drying (at least, for 24 hours)
3. Section the gonads in the microtome Leica RM 2155 with a thickness of 3 µm.
4. Obtain 3 to 5 sections per gonad and collect them with microscope slides.
5. Leave the preparations drying for 24 hours.

D. Staining

1. The preparations are colored with toluidine blue
2. For such purpose, put the microscope slides in a tub with the stain, so that they are completely covered with the stain.
3. After 1 min, rinse with water.
4. Leave it drying for some hours.
5. Glue the cover slip to the microscope slides with Neo-Mount glue. Immerse the lamella in Neo-Clear, put 3 drops of glue in the slide and put the lamella above.
6. Leave it drying for 24 hours.